Fibroblast Growth Factor Receptor 1–5-Hydroxytryptamine 1A Heteroreceptor Complexes and Their Enhancement of Hippocampal Plasticity

D.O. Borroto-Escuela; W. Romero-Fernández; G. Mudó; M. Perez-Alea; F. Ciruela; A.O. Tarakanov; M. Narvaez; V. Di Liberto; L.F. Agnati; N. Belluardo; K. Fuxe

Published article: Borroto-Escuela DO, Romero-Fernández W, Mudó G, Perez-Alea M, Ciruela F, Tarakanov AO, Narvaez M, Di Liberto V, Agnati LF, Belluardo N, Fuxe K. Fibroblast Growth Factor Receptor 1–5-Hydroxytryptamine 1A Heteroreceptor Complexes and Their Enhancement of Hippocampal Plasticity. Biological Psychiatry. 2012;71(1):84–91. doi:10.1016/j.biopsych.2011.09.012.

FGFR1-5-HT1A HETERORECEPTOR COMPLEXES AND THEIR ENHANCEMENT OF HIPPOCAMPAL PLASTICITY

Dasiel O. Borroto-Escuela[a], Wilber Romero-Fernandez[a], Giuseppa Mudó[b] , Mileidys Pérez-Alea[c], Francisco Ciruela[d], Alexander O. Tarakanov[e], Manuel Narvaez[f], Valentina Di Liberto[b] , Luigi F. Agnati[g], Natale Belluardo[b] and Kjell Fuxe[a*]

[a]Department of Neuroscience, Karolinska Institutet, Stockholm, Sweden.

[b]Department of Experimental Biomedicine and Clinical Neurosciences, Laboratory of Molecular Neurobiology, University of Palermo, Palermo, Italy.

[c]School of Life and Health, Aston University, Birmingham, United Kingdom.

[d]Unitat de Farmacologia, Departament Patologia i Terapèutica Experimental, Universitat de Barcelona, Spain.

[e]Russian Academy of Sciences, St. Petersburg Institute for Informatics and Automation, Saint Petersburg, Russia.

[f]Department of Physiology, School of Medicine, University of Málaga, Spain.

[g]IRCCS Lido Venice, Italy.

Corresponding author: Kjell Fuxe, Professor, Retzius väg 8, 17177 Stockholm, Sweden. Tel: +46 8 52487077; Fax: +46 8 315721; E-mail: Kjell.Fuxe@ki.se.

Key words: fibroblast growth factor receptor, serotonin receptors, neuronal plasticity, heteroreceptor, depression, allosteric modulation.

Number of words in the abstract: 249/250

Number of words in the article body: 3973/4000

Figures: 3

Tables: 0

References: 31

Supplemental text information: 34 pages

Abstract

Background: The hippocampus and its 5-HT transmission plays an important role in depression related to its involvement in limbic circuit plasticity.

Methods: The analysis was made with BRET, coimmunoprecipitation, in situ proximity ligation assay (PLA), binding assay, in cell western and gene reporter assay and the forced swim test.

Results: Using BRET analysis, FGFR1-5-HT1A receptor complexes has been demonstrated and their specificity and agonist modulation characterized. The receptor interface involves TM-V and TM-VII and putative helix-8 of the 5-HT1AR. Their presence based on coimmunoprecipitation and PLA has also been indicated in hippocampal cultures and rat dorsal hippocampal formation showing a neuronal location. In vitro assays on ERK1/2 phosphorylation have shown synergistic increases in signaling upon coactivation with FGF-2 and a 5-HT1A agonist which are specific in a pharmacological and siRNA study and dependent on the heteroreceptor interface. In vitro and in vivo studies also revealed a 5-HT1A agonist induced phosphorylation of FGFR1 and ERK1/2 in rat hippocampus without changing FGF-2 levels. Coactivation of the heteroreceptor also resulted in synergistic increases in extensions of PC12 cells and neurite densities and protrusions in primary hippocampal cultures dependent on the receptor interface. The combined acute and repeated i.c.v. treatment with FGF-2 and 8-OH-DPAT was found to produce evidence of highly significant antidepressant actions in the forced swim test.

Conclusion: The findings indicate that neurotrophic and antidepressant effects of 5-HT in brain may in part be mediated by activation of the 5-HT1AR protomer in the hippocampal FGFR1-5-HT1A receptor complex enhancing the FGFR1 signaling.

Introduction

The hippocampal atrophy found in major depression may be involved in the pathophysiology of this disease in view of its critical role in the emotional networks and in behavior (1-5). The atrophy could result from the down-regulation of neurotrophic factors in the hippocampal formation (6), which may also be true for the atrophy in the prefrontal cortex (14). In fact , FGF-2 mRNA levels in the hippocampus are reduced in major depression (7, 8) and this region appears to show an especially strong atrophy (9). Interestingly, treatment with antidepressant drugs in rodents can increase hippocampal FGF-2 levels in rodents (10). Furthermore, intraventricular (i.c.v) injections of FGF-2 produce antidepressant actions in the rat (11).

The therapeutic effect of the most commonly prescribed antidepressants, like the selective serotonin reuptake inhibitors (SSRIs), e.g. fluoxetine and the 5-HT1A partial agonist Buspirone (12-14), may in part be related to the enhancement of 5-hydroxytryptamine (5-HT) neurotransmission in the hippocampus involving mainly the postjunctional 5-HT1A receptor located on the dendrites of the hippocampal glutamate neurons (15). In line with these results a reduced 5-HT1A binding potential has been observed in several brain regions including the hippocampus in major depressive disorder (MDD) (16, 17). Similar reductions in 5-HT1A mRNA levels have been found postmortem in the hippocampus in MDD (18). Increasing evidence exists that treatment with antidepressant drugs, in conjunction with the antidepressant-induced increase in 5HT neurotransmission, could lead to enhanced growth and function of hippocampal neurons by up-regulating expression of neurotrophic factors (3). An involvement of the fibroblast growth factors (FGFs) has been proposed in mood disorders (19) and 5-HT exerts neuroprotective effects (20). In fact, SSRIs and chronic electroconvulsive shock treatment increase FGF-2 expression in the

hippocampus and frontal cortex (10) opening up the possibility that FGF-2 can at least in part mediate the antidepressant effects of SSRI and buspirone treatments. In agreement, FGF-2 is distinctly expressed in astrocyte and nerve cell populations of the hippocampus (21) as is FGFR1, one of its receptors (22).

There exists evidence for the existence of direct (heteromer receptor complexes) and/or indirect G protein coupled receptor (GPCR)-Receptor tyrosine kinase (RTK) interactions which even in the absence of neurotrophic factor binding to the RTK can lead to transactivation of RTKs, which can produce effects on cell proliferation, differentiation and neuronal plasticity (23-26).

Here evidence is given for the existence of FGFR1-5-HT1A heteroreceptor complexes in the rat hippocampus with a partial characterization of their interface. The findings demonstrate their enhancing role in hippocampal plasticity that may be considered to play a role in reversing the depression-induced atrophy of hippocampal neurons.

Methods and Materials

Detailed descriptions are available in Supplementary Material and Methods on: chemicals, reagents and drug administration; antibodies; receptor constructs; cell culture, transfection and RNA interference; transmembrane peptide treatment; membrane preparation and ligand binding assay; *in situ* Proximity Ligation Assay (PLA); immunofluorescence microscopy; immunocytochemistry; co-immunoprecipitation; $BRET^2$ competition and saturation assay; luciferase gene assay; *in cell western* and Western blot analysis in animal tissue preparation; bioinformatic analysis of the receptor-receptor interface; animals and drugs, surgical preparation, acute and repeated i.c.v. injections, forced swim test and behavioral scores.

PC12 cell differentiation

Sterile poly-D-lysine–coated cover slips were used to grow PC12 cells at a density of 2 × 10^5 cells per 10 cm^2. Plated cells were grown in 3 ml of nonsupplemented medium for 24 h. Ligands were added to the cells and incubated at 37 °C for 48 h, new ligands were added to fresh nonsupplemented medium and incubation was continued for 48 h at 37°C. Cells were then fixed with 4% cold paraformaldehyde (wt/vol), the cover slips were mounted on slides and the cells were analyzed. Brightfield images were obtained using an Olympus IX70 with a Q-Fire CCD camera. Average number of extensions per 1000 cells was determined as well as the mean extension lengths from measurement of 100 cells were quantified per condition in three independent experiments; length was converted into micrometer and analyzed for statistical significance using Prism 4.0 (GraphPad, San Diego, CA).

Analysis of neurite density

Cultured hippocampal neurons (7 d *in vitro*) were treated under different pharmacological conditions as indicated and grown for an additional 1 or 24 hour (in the case of siRNA transfections, neurons where transfected 3d before pharmacological treatment). Nerve cells were stained with rabbit anti-MAP2 monoclonal antibody (5 µg/ml; Cell Signalling Tech) and mouse anti-NeuN monoclonal antibody (5 µg/ml; Millipore). Each image was acquired with a Leica SP2 confocal microscope (40×) and consisted of a *z* stack of pictures taken at a depth interval of 0.5 µm and then projected into one image. Acquisition of microscopy images and morphometric quantifications were performed by investigators blind to the experimental condition. After taking images of MAP2-NeuN positive neurons with cell body diameter in the order of 10–20 µm in diameter, three parameters of neurite growth were analyzed: mean neurite density as determined by MAP2 immunoreactivity (neurite field area/number of NeuN positive cells), mean number of MAP2 immunoreactivity protrusions (putative spines) per 100µm of neurite (5 segments of 100µm per nerve cell of

each conditions) and the presence or absence of nerve cells showing growth cones with filopodia and/or lamellipodium. Typically, images of 20-30 neurons per condition were captured for each experiment and four independent experiments were performed. The application settings were adjusted at the beginning of analysis and kept the same for all images in the experiment.

Data analysis

The number of samples (*n*) in each experimental condition is indicated in Figure legends. All data were analyzed using the commercial program Prism 4.0 (GraphPad, San Diego, CA). When two experimental conditions were compared, statistical analysis was performed using an unpaired *t* test. Otherwise, statistical analysis was performed by one-way analysis of variance (ANOVA) followed by Tukey's Multiple Comparison post-test. The *P* value 0.05 and lower was considered significant. $^{*}P<0.05$, $^{**}P<0.01$, $^{***}P<0.001$. BRET isotherms were fitted using a nonlinear regression equation assuming a single binding site, which provided BRETmax and BRET50 values. The correlation between fluorescence or luminescence and receptor density was analyzed by a linear regression curve fitting with the same software.

Results

FGFR1- 5-HT1A heteroreceptor complexes and their receptor interface

Hippocampal tissue (rat). In Fig.1A nerve cells of the pyramidal cell layer of CA1 and CA3 of the dorsal hippocampus are shown to be positive with the proximity ligation assay (PLA) having many red clusters. PLA positive nerve cells are also found in the dorsal leaflet of the dentate gyrus (dDG) and CA4, but are absent in the cerebral cortex, the corpus callosum and the ventral leaflet of DG (Supplementary Fig.S1D). FGFR1 and 5-

HT1A receptors were found to coimmunoprecipitate in rat dorsal hippocampus (Fig.1B) in line with the results obtained with the PLA.

Primary hippocampal cultures. The neuronal FGFR1-5-HT1A receptor complexes were also demonstrated with PLA and the mean number of red clusters per cell was found to be significantly increased by FGF-2 or 8-OH-DPAT treatment alone with a significantly enhanced increase upon combined treatment (Fig.1C).The colocalization of FGFR1 and 5-HT1A receptors was studied by transient cotransfection with 5-HT1A-YFP and FGFR-GFP2 (Supplementary Fig.S2A). Partial colocalization was shown through appearance of yellow-orange fluorescence in the plasma membrane, especially of the neurites of the hippocampal nerve cells.

HEK293T cells. After transient cotransfection of FGFR1 and 5-HT1A similar red cluster numbers per cell were observed as in the hippocampal cultures (Supplementary Fig.S1B-b1). Again an increase in the PLA signal was observed after FGF-2 or 8-OH-DPAT alone, which was significantly enhanced by combined treatment (Supplementary Fig.S1B-b1). As in the case of primary hippocampal cultures transient cotransfection with 5-HT1A-YFP and FGFR-GFP2 demonstrated colocalization as seen from the appearance of the yellow fluorescence in the plasma membrane (Supplementary Fig.S2B). With confocal microscopy of the cotransfected HEK293T cells a cointernalization of 5-HT1A-YFP and FGFR1-GFP2 was demonstrated after FGF-2, 8-OH-DPAT and especially after their combined treatment (Supplementary Fig.S2B).

The $BRET^2$ analysis standard curves were used to convert fluorescence and luminescence values into fmoles/mg protein of receptor in order to obtain accurate Bmax and BRET50 values (Supplementary Fig.S3A). The $BRET^2$ studies in HEK293T cells demonstrated a specific interaction between 5-HT1A and FGFR1 (saturation curve) while cotransfection of FGFR1 and 5-HT2A (negative control) led only to a linear regression and thus these

receptors failed to specifically interact (Fig.1D). 5-HT2A and 5-HT2C unlike 5-HT1A and 5-HT1B also failed to compete with the formation of the FGFR1-5-HT1A heteroreceptor complex (Fig.1D). The specificity is again shown by the observation that TrkA failed to reduce the $BRET^2$ ratio in competition experiments (Supplementary Fig.S3B). Treatment with FGF-2 or 8-OH-DPAT significantly reduced the BRET50 values and thus increased the affinity of the FGFR1-5-HT1A heteroreceptor interaction (Fig.1D).This action was significantly enhanced by combined treatment when compared with the 8-OH-DPAT but not the FGF-2 alone group (Fig.1D). When not expressing the $BRET^2$ ratio in percent of maximal response, the combined treatment with 8-OH-DPAT and FGF-2 can be seen to substantially increase the BRETmax values (Supplementary Fig.S3C) indicating that the combined treatment substantially increases the recruitment of the FGFR1-5-HT1A heteroreceptor complex.

To study the FGFR1-5-HT1A receptor interface, $BRET^2$ ratio competition with TMII, TMV and TMVII of the 5-HT1A receptor was performed (Fig.1E). TMV and TMVII gave increase to full competition curves starting around 10 nM and with no $BRET^2$ signal remaining at 1000 nM. TMII was substantially less effective and had a very low potency. The other TM peptides were totally ineffective, with the exception of small significant reduction with TMIV (Fig.1E). In the interface analysis also a 5-HT1A receptor with a deleted helix8 (5-HT1A-Hx8) was used, since 3D molecular modeling indicated that this domain may potentially interact with the intracellular domains of FGFR1 (Supplementary Fig.S4A, see also (26)).This mutated 5-HT1A receptor was expressed at the cell surface and had an intact ability to bind the 5-HT1A agonist 8-OH-DPAT and to inhibit the forskolin-induced cAMP formation and increase SRE transcription (Supplementary Fig.S4A-B). In the $BRET^2$ analysis the 5-HT1A-Hx8 showed an increased BRET50 value vs the WT receptor and a significantly reduced ability to compete for the formation of the

FGFR1-5-HT1A receptor complex vs the WT 5-HT1A receptor (Supplementary Fig.S4C). Thus, this mutated 5-HT1A receptor has a reduced ability to form a receptor complex with FGFR1.

Bioinformatics. Based on a mathematical approach, a set of triplet amino acid homologies has been deduced that may be responsible for receptor-receptor interactions. The triplets AAR and ARE that may involve electrostatic interactions between AAR-ARE may participate in the formation of the FGFR1-5HT1A heteroreceptor complex through 'guide-clasp' protein-protein interactions (Supplementary Fig.S5).

FGFR1 transactivation, ERK1/2 phosphorylation and hippocampal plasticity in primary hippocampal cultures

FGFR1 transactivation. To evaluate the 5-HT1A agonist induced transactivation of the FGFR1, 8-OH-DPAT induced phosphorylation of FGFR1 (pFGFR1) was studied in concentration response and time course experiments (Fig.2A). The peak increase of pFGFR1 was observed at 0.5 μM followed by a disappearance of the response with increasing concentrations of the 5-HT1A agonist and in the time-course the maximal increase was already observed at 2.5-5 min and was still maximally developed at 20 min. The 5-HT1A agonist induced increase of pFGFR1 was blocked by FGFR1 inhibitors and by a 5-HT1A receptor antagonist (Supplementary Fig.6A). The 5-HT2A agonist DOI failed to increase pFGFR1 levels (Supplementary Fig.6C).

ERK1/2 phosphorylation. The consequences of the 5-HT1A induced increase in pFGFR1 on its signaling were studied by analysis of single and combined FGF-2 and 8-OH-DPAT treatment on ERK1/2 phosphorylation (Fig.2B, Supplementary Fig.S6D). A marked synergistic increase in ERK1/2 phosphorylation was observed after the combined treatment starting already after 5 min and was still maintained after 120 min. Also 8-OH-DPAT was found to increase the potency of FGF-2 in a concentration dependent way (50-300 nM)

(Fig. 2B). Treatment with 8-OH-DPAT alone in concentration-response and time-course experiments on ERK1/2 phosphorylation matched its ability to increase pFGFR1 with an expected slight delay (Fig. 2B, Supplementary Fig.S6D). The synergistic increase of pERK1/2 by combined FGF-2 and 5-HT1A agonist treatment was blocked by FGFR1 inhibitors and by the 5-HT1A antagonist (Fig.2C and Supplementary Fig.S6B) and in siRNAfgfr1 or siRNA5ht1a transfected cells (Fig.2C and Supplementary Fig.S7A-C).

The receptor interface of the FGFR1-5-HT1A receptor complex appeared to be crucial for this synergism since it was counteracted by incubation with TMV and TMVII of the 5-HT1A receptor (Fig.2C). In experiments with 8-OH-DPAT alone in primary hippocampal cultures the increase in pERK1/2 produced by the 5-HT1A agonist was blocked not only by the 5-HT1A antagonist but also by the FGFR1 inhibitors (Fig. 2C). Thus, the 5-HT1A agonist induced increase appears to be dependent on transactivation of the FGFR1 likely taking place over the receptor interface of the FGFR1-5-HT1A heteroreceptor complex.

pERK1/2 and Rab5 colocalization (marker of early endosomes) (Supplementary Fig. S6E,S6E-A and -B). After FGF-2 (0.05 ug/ml) but not after 8-OH-DPAT (0.25 uM) there was a significant increase in punctate pERK1/2 immunoreactivity (IR, in green fluorescence) colocated with Rab5-RFP at 30 and 120 min measured as an increase in yellow fluorescence intensity or as an increase in the ratio of yellow fluorescence intensity to total pERK1/2 green fluorescence intensity (Supplementary S6E-A). Also the mean number of early endosomes (pERK1/2-IR-Rab5-RFP) per cell was significantly increased (Supplementary S6E-B). The increase in these parameters became markedly enhanced and highly significant by cotreatment with FGF-2 and 8-OH-DPAT (Supplementary Fig.S6E, S6E-A and -B). At 120 min after combined treatment the punctate bodies of yellow fluorescence (pERK1/2-IR green-Rab5-RFP) in early endosomes had reached a distinct perinuclear location (Supplementary Fig. S6E).

Neuronal plasticity. To obtain a morphological correlation to the synergistic increase of pERK1/2 with FGF-2 and the 5-HT1A agonist, effects of this combined treatment has been studied on extensions from PC12 cells and on neurite density and protrusions in primary hippocampal cultures. In Fig.2D-D1 it is demonstrated that this combined treatment produced a highly significant increase in the number of extensions per 1000 PC12 cells after a 4 day incubation. This increase is blocked not only by FGFR1 inhibitors and by the 5-HT1A antagonist but also by TMV and TMVII incubation, while TMII is ineffective (for further details, see Supplementary Fig.S8A-C).

The results on neurite density in primary hippocampal cultures are shown in Fig.2E-E1 and Supplementary Fig.S9A-B. There is a synergistic and highly significant increase of mean neurite density per 100 cells upon coactivation of the two receptors for 24 h as shown with MAP2 immunocytochemistry and image analysis. The synergic effects are fully blocked by a FGFR1 inhibitor and a 5-HT1A antagonist and markedly reduced by incubation with TMV and TMVII but not with TMII (Fig.2E1). Transfection of the cells with siRNAfgfr1 and siRNA5ht1a gives a full blockade of the increase of neurite density by cotreatment with FGF-2 and 8-OH-DPAT (Supplementary Fig.S9A-B). There is also a synergistic increase of protrusions (putative spines) from neurites of the primary hippocampal nerve cells upon a 1 h treatment with FGF-2 and the 5-HT1A receptor agonist as shown with MAP2 immunocytochemistry (Fig.2F).

This plasticity action is again fully blocked by a FGFR1 inhibitor and a 5-HT1A receptor antagonist and markedly reduced by incubation with TMV and TMVII but not with TMII for 1h (Fig.2F1). Finally, 1 h incubation with both FGF-2 and a 5-HT1A receptor agonist but not with either alone produced a development of growth cones displaying high numbers of filopodia and a distinct lamellopodium in the primary hippocampal cultures (Fig.2G).

Hippocampal FGFR1 transactivation and ERK1/2 phosphorylation after in vivo treatment with FGF-2 and 8-OH-DPAT

In vivo results have been obtained by exploring the effects of intraventricular treatment with 8-OH-DPAT and/or FGF-2 on pFGFR1 and pERK1/2 levels in the rat dorsal hippocampus (Fig.3A-B). Upon combined intraventricular treatment with 8-OH-DPAT and FGF-2 a synergistic and significant increase of phosphorylation of FGFR1 and ERK1/2 was observed at 6h, 12h and 24h in the rat hippocampus. The systemic 5-HT1A receptor agonist treatment produced a significant increase of the phosphorylation of both FGFR1 and ERK1/2 in the dorsal hippocampus but not in the cerebral cortex (Fig.3C-D) without a change in the hippocampal levels of FGF-2 (Supplementary Fig.S10).

Behavioural effects of i.c.v. treatment with FGF-2 and/or 8-OH-DPAT in the forced swim test

The effects of acute and a 10 day treatment are shown 24 h after the treatment in Fig.3E. Acute experiment (upper panel): The combined treatment gives a substantial and highly significant reduction in immobility time and increase in swim time compared with the vehicle group and the FGF-2 and 8-OH-DPAT alone groups. FGF-2 alone but not 8-OH-DPAT produces a small but significant reduction of immobility and increase in swim time compared with vehicle. Climb time was not affected by any treatment.

10 day experiment (lower panel): Combined repeated i.c.v. treatment (24 h after last injection) gives a substantial and highly significant reduction in immobility time and increase in swim time compared with the vehicle group and the FGF-2 and 8-OH-DPAT alone groups. FGF-2 alone but not 8-OH-DPAT produces a small but significant reduction of immobility and increase in swim time compared with the vehicle group. Swim time in the FGF-2 alone group was also significantly different from the swim time in the 8-OH-DPAT alone group.

Discussion

The findings of this study give the first evidence that there exists in the rat hippocampus a FGFR1-5-HT1A heteroreceptor complex using the PLA and coimmunoprecipitation techniques, which we have previously proposed to exist (8). The results also show it plays a significant role in hippocampal plasticity. In 2008 an A2A-FGFR1 receptor complex was discovered using the yeast two-hybrid system where FGF acts as a cotransmitter to regulate synaptic plasticity (6). Our heteroreceptor complex was also demonstrated with the PLA in primary hippocampal cultures and HEK293T cells transiently cotransfected with FGFR1 and 5-HT1A. Especially combined treatment with FGF-2 and 8-OH-DPAT increased the number of clusters per cell with the PLA suggesting agonist induced increases in the formation of the FGFR1-5HT1A heteroreceptor complexes. Evidence for the existence of such complexes was also obtained with the $BRET^2$ technique in HEK293T cells. Again an agonist regulation was observed especially after combined agonist treatment leading to an increase in the affinity of the interaction of the two receptor protomers and in the number of receptor complexes formed. The specificity of the receptor complex formation in HEK293T cells with the $BRET^2$ technique was also demonstrated together with the colocalization and cointernalization of the two receptors using $FGFR1^{GFP2}$ and $5\text{-}HT1A^{YFP}$. TMV and TMVII of the 5-HT1A were shown to be part of the interface of this heteroreceptor complex based on $BRET^2$ competition assays. The helix8 of the 5-HT1A may also contribute to the interface since the 5-HT1A receptor with a deleted Hx8 had a reduced affinity to form a heteroreceptor complex with FGFR1.

Evidence for a significant impact of the FGFR1-5-HT1A heteroreceptor complex on hippocampal plasticity was obtained in the studies on primary hippocampal cultures. Here the 5-HT1A agonist produced a rapid and concentration dependent transactivation of

FGFR1 as seen from its increased phosphorylation. Furthermore, a rapid, specific and marked synergistic increase in ERK1/2 phosphorylation was observed upon cotreatment with FGF-2 and 8-OH-DPAT found to be dependent on the receptor interface in incubation experiments with TMV and TMVII. In addition, the 5-HT1A agonist increased the FGF-2 potency to produce increases in ERK1/2 phosphorylation. This synergistic increase in pERK1/2 upon cotreatment may involve an increased phosphorylation of ERK1/2 in early endosomes in view of its markedly increased colocation with the early endosome marker Rab5-RFP. In addition, pERK1/2 due to its link to early endosomes is transferred into a perinuclear position which may facilitate its entry into the nucleus and contribute to enhanced effects of pERK1/2 on gene expression.

A major result was the evidence obtained that these transactivation and signaling events in the FGFR1-5-HT1A heteromer could be linked to rapid and marked synergistic increases of neurite density (24h), protrusions and growth cone (1h) development in the hippocampal cultures. The plasticity phenomena in neurite density and protrusions (putative spines) as well as the marked increase in extensions from PC12 cells were found to be strongly counteracted by preincubation with TMV and TMVII of the 5-HT1A receptor, shown to be part of the interface of this heteroreceptor complex.

Another major result was the in vivo finding that intraventricular injections of FGF-2 and 8-OH-DPAT in the rat produced synergistic and prolonged increases in the FGFR1 and ERK1/2 phosphorylation levels in the hippocampus. Thus, it seems likely that synergistic increases in neurite density and protrusions may also develop in the hippocampus in vivo upon coactivation of the protomers of the hippocampal FGFR1-5-HT1A heteroreceptor complex. In support of this view systemic treatment with the 5-HT receptor agonist produced a transactivation of hippocampal FGFR1 receptor as seen from the significant increase in FGFR1 and ERK1/2 phosphorylation levels 24 h later. A regional selectivity

was also observed, since no FGFR1 transactivation was observed in the cerebral cortex which is in line with our failure to observe PLA positive clusters in the cerebral cortex indicating a marked reduction of FGFR1-5-HT1A heteroreceptor complexes in this region in spite of codistribution of the two receptor systems in the cerebral cortex (27). The two receptors could be targeted to different domains of the plasma membrane and/or have a higher affinity to interact with other receptor proteins in this region.

The combined acute i.c.v. treatment with FGF-2 and 8-OH-DPAT as performed in the analysis of neuronal plasticity was found to produce strong indications of acute antidepressant actions in the forced swim test as evidenced from the substantial reductions in immobility time and increases in swim time without changes in climb time. The molecular mechanism may involve a 5-HT1A agonist induced enhancement of the FGFR1 signaling in the FGFR1-5-HT1A heteroreceptor complex in the hippocampus via an allosteric facilitatory receptor-receptor interaction. In this way the acute weak antidepressant actions of FGF-2 become more robust and highly significant. Combined repeated i.c.v. treatment with FGF-2 and 8-OH-DPAT over 10 days produced strong indications of maintained antidepressant actions failing to develop desensitization in the forced swim test as evidenced from maintained substantial reductions in immobility time and increases in swim time without changes in climb time.

Finally, our findings may be considered to give a new molecular basis for the therapeutic actions of antidepressant drugs like SSRIs or 5-HT1A receptor agonists (12-14, 16, 17). It may be proposed to involve a 5-HT induced transactivation of FGFR1 in the discovered hippocampal FGFR1-5-HT1A heteroreceptor complex helping to reverse the depression-induced atrophy of hippocampal neurons.

It is true that SSRIs only produce antidepressant effects after a delay of several weeks (19), while the hippocampal plasticity increase and the antidepressant effects observed here in

the forced swim test rapidly develops upon coactivation of the two receptors in the FGFR1-5-HT1A heteroreceptor complex. The serotonin receptor subtype disbalance hypothesis of depression may help explain this delay seen with SSRIs (28, 29). Thus, certain 5-HT receptor subtypes like 5-HT1A receptors favour mood elevation while others like 5-HT2A receptor subtypes may favour a depressed mood. Treatment with SSRIs with elevation of extracellular 5-HT levels may only produce antidepressant actions when after a time delay the proper balance of the activities of the different 5-HT receptor subtypes has been obtained favouring the activity in the mood elevating 5-HT receptor subtypes through differential adaptive changes. It seems possible that with SSRIs the allosteric facilitatory receptor-receptor interaction in FGFR1-5-HT1A heteroreceptor complexes only becomes enhanced upon weeks of treatment. The selective activation of the 5-HT1A subtype together with FGFR1 activation can lead to more rapid and robust antidepressant effects as observed in the forced swim test. Rapid antidepressant effects have previously been observed with N-methyl-D-aspartate glutamate receptor antagonists like ketamine (30). Thus, there appears to be a link to serotonin based pharmacological interventions.

The explanation given above is compatible with reports that both acute and chronic treatments with FGF-2 given i.c.v in rats have been shown to produce anti-depressant-like actions (11). Furthermore, both hippocampal FGF-2 and FGFR1 mRNA levels are downregulated following acute social defeat (31). This hippocampal heteroreceptor complex, therefore, may be proposed to be a novel target for anti-depressant drug development through which more rapid and robust antidepressant actions may potentially develop.

Acknowledgements

This work has been supported by the Torsten and Ragnar Söderberg Foundation, Stockholm, Sweden. A.O.T. has not received any support for this work.

Financial disclosures

The authors report no biomedical financial interests or potential conflicts of interest.

REFERENCES

1. Rajkowska G, Miguel-Hidalgo JJ, Wei J, Dilley G, Pittman SD, Meltzer HY, Overholser JC, Roth BL, Stockmeier CA (1999): Morphometric evidence for neuronal and glial prefrontal cell pathology in major depression. Biol Psychiatry 45: 1085-1098
2. Castren E, Voikar V, Rantamaki T (2007): Role of neurotrophic factors in depression. Curr Opin Pharmacol 7: 18-21
3. Schmidt HD, Duman RS (2007): The role of neurotrophic factors in adult hippocampal neurogenesis, antidepressant treatments and animal models of depressive-like behavior. Behav Pharmacol 18: 391-418
4. Sheline YI (1996): Hippocampal atrophy in major depression: a result of depression-induced neurotoxicity? Mol Psychiatry 1: 298-299
5. McEwen BS (1999): Stress and hippocampal plasticity. Annu Rev Neurosci 22: 105-122
6. Charney DSN, Eric J. (2008) Neurobiology of Mental Illness, 3rd edn. Oxford University Press, Oxford
7. Evans SJ, Choudary PV, Neal CR, Li JZ, Vawter MP, Tomita H, Lopez JF, Thompson RC, Meng F, Stead JD, Walsh DM, Myers RM, Bunney WE, Watson SJ, Jones EG, Akil H (2004): Dysregulation of the fibroblast growth factor system in major depression. Proc Natl Acad Sci U S A 101: 15506-15511
8. Gaughran F, Payne J, Sedgwick PM, Cotter D, Berry M (2006): Hippocampal FGF-2 and FGFR1 mRNA expression in major depression, schizophrenia and bipolar disorder. Brain Res Bull 70: 221-227
9. Campbell S, Marriott M, Nahmias C, MacQueen GM (2004): Lower hippocampal volume in patients suffering from depression: a meta-analysis. Am J Psychiatry 161: 598-607
10. Mallei A, Shi B, Mocchetti I (2002): Antidepressant treatments induce the expression of basic fibroblast growth factor in cortical and hippocampal neurons. Mol Pharmacol 61: 1017-1024
11. Turner CA, Gula EL, Taylor LP, Watson SJ, Akil H (2008): Antidepressant-like effects of intracerebroventricular FGF2 in rats. Brain Res 1224: 63-68
12. Carlsson A, Fuxe K, Ungerstedt U (1968): The effect of imipramine on central 5-hydroxytryptamine neurons. J Pharm Pharmacol 20: 150-151
13. Wong DT, Bymaster FP, Engleman EA (1995): Prozac (fluoxetine, Lilly 110140), the first selective serotonin uptake inhibitor and an antidepressant drug: twenty years since its first publication. Life Sci 57: 411-441
14. Robinson DS, Rickels K, Feighner J, Fabre LF, Jr., Gammans RE, Shrotriya RC, Alms DR, Andary JJ, Messina ME (1990): Clinical effects of the 5-HT1A partial agonists in depression: a composite analysis of buspirone in the treatment of depression. J Clin Psychopharmacol 10: 67S-76S
15. Riad M, Zimmer L, Rbah L, Watkins KC, Hamon M, Descarries L (2004): Acute treatment with the antidepressant fluoxetine internalizes 5-HT1A

autoreceptors and reduces the in vivo binding of the PET radioligand [18F]MPPF in the nucleus raphe dorsalis of rat. J Neurosci 24: 5420-5426
16. Drevets WC, Thase ME, Moses-Kolko EL, Price J, Frank E, Kupfer DJ, Mathis C (2007): Serotonin-1A receptor imaging in recurrent depression: replication and literature review. Nucl Med Biol 34: 865-877
17. Savitz J, Lucki I, Drevets WC (2009): 5-HT(1A) receptor function in major depressive disorder. Prog Neurobiol 88: 17-31
18. Lopez JF, Chalmers DT, Little KY, Watson SJ (1998): A.E. Bennett Research Award. Regulation of serotonin1A, glucocorticoid, and mineralocorticoid receptor in rat and human hippocampus: implications for the neurobiology of depression. Biol Psychiatry 43: 547-573
19. Turner CA, Akil H, Watson SJ, Evans SJ (2006): The fibroblast growth factor system and mood disorders. Biol Psychiatry 59: 1128-1135
20. Lesch KP (2001): Serotonergic gene expression and depression: implications for developing novel antidepressants. J Affect Disord 62: 57-76
21. Fuxe K, Tinner B, Zoli M, Pettersson RF, Baird A, Biagini G, Chadi G, Agnati LF (1996): Computer-assisted mapping of basic fibroblast growth factor immunoreactive nerve cell populations in the rat brain. J Chem Neuroanat 11: 13-35
22. Belluardo N, Wu G, Mudo G, Hansson AC, Pettersson R, Fuxe K (1997): Comparative localization of fibroblast growth factor receptor-1, -2, and -3 mRNAs in the rat brain: in situ hybridization analysis. J Comp Neurol 379: 226-246
23. Luttrell LM, Daaka Y, Lefkowitz RJ (1999): Regulation of tyrosine kinase cascades by G-protein-coupled receptors. Curr Opin Cell Biol 11: 177-183
24. Lee FS, Chao MV (2001): Activation of Trk neurotrophin receptors in the absence of neurotrophins. Proc Natl Acad Sci U S A 98: 3555-3560
25. Fuxe K, Dahlstrom A, Hoistad M, Marcellino D, Jansson A, Rivera A, Diaz-Cabiale Z, Jacobsen K, Tinner-Staines B, Hagman B, Leo G, Staines W, Guidolin D, Kehr J, Genedani S, Belluardo N, Agnati LF (2007): From the Golgi-Cajal mapping to the transmitter-based characterization of the neuronal networks leading to two modes of brain communication: wiring and volume transmission. Brain Res Rev 55: 17-54
26. Flajolet M, Wang Z, Futter M, Shen W, Nuangchamnong N, Bendor J, Wallach I, Nairn AC, Surmeier DJ, Greengard P (2008): FGF acts as a co-transmitter through adenosine A(2A) receptor to regulate synaptic plasticity. Nat Neurosci 11: 1402-1409
27. Pazos A, Palacios JM (1985): Quantitative autoradiographic mapping of serotonin receptors in the rat brain. I. Serotonin-1 receptors. Brain Res 346: 205-230
28. Fuxe K, Hedlund P, von Euler G, Lundgren K, Martire M, Ogren S, Eneroth P, Agnati L (1991) Galanin/5-HT interactions in the rat central nervous system. Relevance for depression. In: Hökfelt T, Bartfai T, Jacobowitz D, Ottoson D (eds) Galanin A new multifunctional peptide in the neuroendocrine system. Wenner-Gren Center International Series, London, pp 221-235
29. Fuxe K, Ogren SO, Agnati L, Gustafsson JA, Jonsson G (1977): On the mechanism of action of the antidepressant drugs amitriptyline and nortriptyline. Evidence for 5-hydroxytryptamine receptor blocking activity. Neurosci Lett 6: 339-343
30. Krystal JH N-methyl-D-aspartate glutamate receptor antagonists and the promise of rapid-acting antidepressants. Arch Gen Psychiatry 67: 1110-1111

31. Turner CA, Calvo N, Frost DO, Akil H, Watson SJ (2008): The fibroblast growth factor system is downregulated following social defeat. Neurosci Lett 430: 147-150

Figure legends

Figure 1. FGFR1 and 5-HT1A heteroreceptor complexes colocalize and interact. (A) Detection of FGFR1-5-HT1A heteroreceptor complexes (seen as red clusters indicated by arrows) in dorsal rat hippocampus by *in situ* PLA. Scale bars, 10 μm (top) and 50 μm (bottom). **(B)** Specific coimmunoprecipitation of FGFR1 and 5-HT1A in rat hippocampal tissue. IB, immunoblot; IP, immunoprecipitation. **(C)** Increased FGFR1-5-HT1A heteroreceptor complex formation upon receptor coactivation in rat primary hippocampal cultures. Cells were treated from day 5 to day 7 with vehicle (-), 8-OH-DPAT (100nM), FGF-2 (50ng/ml) or combined 8-OH-DPAT+FGF-2 (100nM and 50ng/ml, respectively). Growth factors were added a new every day and samples were processed for detection of *in situ* PLA signals. Scale bar=75μm. Quantification of receptor complexes as red clusters/DAPI-positive nuclei in constant sampled fields were determined. Data are means ± s.e.m. (n=6). 8-OH-DPAT (100nM), FGF-2 (50ng/ml) or combined 8-OH-DPAT+FGF-2 groups are significantly different compared to vehicle (***: P<0.001) and combined 8-OH-DPAT+FGF-2 group is significantly different compared to 8-OH-DPAT (100nM) and FGF-2 (50ng/ml) alone group (+++: P<0.001). **(D-top)** $BRET^2$ shows specific 5-HT1A and FGFR1 interaction in HEK293T cells. $BRET^2$ saturation curves were generated in HEK293T cells expressing a fixed amount of FGFR1-Rluc and increasing amounts of 5-HT1A-GFP2 or 5HT2A-GFP2. Cells were pre-incubated 10 min with vehicle, 8-OH-DPAT (100 nM), FGF-2 (50ng/ml), or with both 8-OH-DPAT and FGF-2 (100nM and 50ng/ml). The BRET50 values were significantly reduced by combined, 8-OH-DPAT and FGF-2 treatment alone versus vehicle (P<0.001); 8-OH-

DPAT treatment was significantly different versus combined treatment and FGF-2 treatment alone (P<0.01). The 5-HT1A/FGFR1 curve fitted better to a saturation curve than to a linear regression (5HT2A/FGFR1), F test ($P < 0.001$). Data are means ± s.e.m. (n=8). **(D-bottom)** 5-HT1A and 5HT1B specifically interact with FGFR1 as seen from the competition curves. Data are means ± s.e.m. (n=5). Asterisks indicate the degree of significance between 5-HT1A/1B versus 5HT2A/2C groups ($^{***}P$<0.001; starting from 4.0μg cDNA). **(E)** TMV/VII of 5-HT1A can fully compete with the FGFR1-5-HT1A heteroreceptor complex. The effect of different TM peptides of 5-HT1A on $BRET^2$ signals is shown. Values represent percentages of maximal saturable $BRET^2$ signals. Mean ± s.e.m (n=4). Asterisks indicate the degree of significance compared with control ($^{***}P$<0.001, $^{*}P$<0.001).

Figure 2. FGFR1-5-HT1A receptor-receptor interactions involving FGFR1 transactivation, ERK1/2 phosphorylation and hippocampal plasticity. (A) 8-OH-DPAT-stimulated FGFR1 tyrosine kinases phosphorylation in primary hippocampal cultures. Data are mean ± s.e.m, n=3. **(B-above)** Synergistic activation of the ERK1/2 phosphorylation is induced by coactivation of 5-HT1A and FGFR1 in rat primary hippocampal cultures. Time-course of ERK1/2 phosphorylation was significantly different between the combined group and FGF-2 alone and 8-OH-DPAT alone (P<0.001); a significant different between FGF-2 versus 8-OH-DPAT was observed at 10-45 min (P<0.05). Data are mean ± s.e.m, n=5. **(B-below)** 8-OH-DPAT concentrations dependently shift the FGF-2 concentration responses to the left (P<0.001; as seen from EC50 values) at 10 min of agonist incubation. **(C-left)** Synergistic activation of the ERK1/2 phosphorylation is block by the 5-HT1A TM peptide V and VII. The following concentration were used; (8-OH-DPAT (100nM), FGF-2 (5ng/ml), PD173074 (60nM), S-WAY10013 (1μM) and each TM (0.4μM)). Combined treatment group is significantly

different from 8-0H-DPAT and FGF-2 alone (P<0.001); the groups with TM peptides, 5-HT1A antagonist and FGFR1 inhibitor are significantly different from the combined treatment group (P<0.001). **(C-right)** Again the 5-HT1A antagonist and ERK1/2 inhibitor treated group as well as the siRNA^{fgfr1} and siRNA^{5ht1a} groups markedly block the synergistic effect of the combined treatment group (P<0.001). The following concentration were used; (8-OH-DPAT (100nM), FGF-2 (5ng/ml), PD173074 (60nM), S-WAY10013 (1μM) and each TM (0.4μM)). Data are mean ± s.e.m, n=5. **(D)** 5-HT1A markedly enhanced FGF-2-mediated neurite outgrowth in PC12 cells. Serum-starved PC12 cells were treated without (Control) or with FGF-2 (50ng/ml) and/or 8-OH-DPAT (100nM), in the presence or absences of PD173074 (60nM) or S-WAY100135 (1μM) as indicated. Each 24h, the medium was replaced and fresh ligands were added. After a total incubation time of 4 d, the cells were fixed and photographed. Extensions were analyzed under light microscopy. Average number of extensions divided by 1,000 cells. The quantification is seen in d1 where the data are presented as mean ± s.e.m. The combined group is significantly different from 8-OH-DPAT and FGF-2 alone (***P<0.001); the groups treated with TM peptide, FGFR1 inhibitor and 5-HT1A antagonist are highly significantly reduced versus the combined treated group (***P<0.001, $^{++}$ P<0.01). **(E)** FGFR1-5-HT1A agonists modulation of density of neurites. Primary hippocampal neurons, starved for 3 h, were treated for 60 min without (Control) or with FGF-2 (50ng ml-1) and/or 8-OH-DPAT (100nM). The numbers of neurites/cell were determined after immunofluorescent labeling of neurites and neuronal nuclei (MAP2/NeuN). Quantification is presented in e1 where the data are presented as mean ± s.e.m. The combined group is significantly different from 8-OH-DPAT and FGF-2 alone (***P<0.001); the groups treated with TM peptide, FGFR1 inhibitor and 5-HT1A antagonist are highly significantly reduced versus the combined treated group (***P<0.001, $^{++}$ P<0.01). **(F)** The number of protrusions in neurites/cell

were determined after immunofluorescent labelling. The marked development of protrusions by combined treatment was blocked by 5-HT1A antagonist (S-WAY 100163) and the FGFR1 inhibitor (PD173064) and by TM-V/VII but not by TM-II. Quantitation is presented in f1 where the data are presented as mean ± s.e.m. The combined group is significantly different from 8-OH-DPAT and FGF-2 alone (***P<0.001); the groups treated with TM peptide, FGFR1 inhibitor and 5-HT1A antagonist are highly significantly reduced versus the combined treated group (***P<0.001, $^{++}$ P<0.01). **(G)** Hippocampal primary cultures stained with MAP2/NeuN immunocytochemistry. Examples of the three different treatments. The combined treatment (1h) with FGF-2 (50ng/ml) and 8-OH-DPAT (100nM) is the only treatment producing a marked development of large growth cones with distinct filopodia and lamellipodium not found neither with FGF-2 (50ng/ml) and 8-OH-DPAT (100nM) alone nor with vehicle. Scale bar represents 20 μm.

Figure 3. Hippocampal FGFR1 transactivation and ERK1/2 phosphorylation and antidepressant effects in the forced swim test after in vivo treatment with FGF-2 and 8-OH-DPAT. (A-B) Synergistic activation of ERK1/2 phosphorylation and FGFR1 phosphorylation in the rat hippocampus after i.c.v co-injection of FGF-2 (50 ng) and/or 8-OH-DPAT (200nmoles). Data are mean ± s.e.m (see Supplementary Material "Animals and drugs" Experiment-2). Three rats per group (total of 12 groups). Combined treated group is significantly different from FGF-2 and 8-OH-DPAT alone group at the time points studied (P<0.01, P<0.05); at six hours the FGF-2 alone group was significantly different from 8-OH-DPAT alone group (P<0.05). Statistical analysis was performed by one-way analysis of variance (ANOVA) followed by Tukey's Multiple Comparison post-test. The P value 0.05 and lower was considered significant. $^{*}P$<0.05, $^{**}P$<0.01, $^{***}P$<0.001. **(C-D)** In vivo FGFR1 transactivation and ERK1/2 phosphorylation in the rat dorsal hippocampus have

been obtained by systemic treatment with 8-OH-DPAT (0.2 mg/kg, ip; 24 h before killing). (C) The 5-HT receptor 1A agonist produced a significant increase of the pFGFR1 in the dorsal hippocampus without a change of pFGFR1 in the frontal cerebral cortex. (D) The 5HT1A agonist induced increase in ERK1/2 phosphorylation matched its ability to increase pFGFR1 in the hippocampus. Like phosphorylation levels of FGFR1, the ERK1/2 phosphorylation in the frontal cerebral cortex did not change after treatment with the 5HT receptor 1A agonist. Statistical analysis was performed by one-way analysis of variance (ANOVA) followed by Tukey's Multiple Comparison post-test. The *P* value 0.05 and lower was considered significant. **(E-top)** Effects of acute i.c.v. injections of FGF2, 8-OH-DPAT and FGF-2 + 8-OH-DPAT on immobility, swim and climb times in the forced swim test 24h after the i.c.v. treatments. The data are presented as means ± s.e.m (n = 5). The combined group is significantly different from 8-OH-DPAT and FGF-2 alone groups (+++P<0.001); the groups treated with FGF-2 alone and the combined treated group are highly significantly reduced versus the vehicle group (*P<0.05, ***P<0.001, respectively). Statistical analysis was performed by one-way analysis of variance (ANOVA) followed by Tukey's Multiple Comparison post-test. **(E-bottom)** Effects of repeated daily i.c.v. injections (10 days) of FGF2, 8-OH-DPAT and FGF-2+8-OH-DPAT on immobility, swim and climb times in the forced swim test 24h after the last i.c.v. injections. The data are presented as mean ± s.e.m (n=5). Immobility: the combined group is significantly different from 8-OH-DPAT and FGF-2 alone groups (+++P<0.001); the groups treated with FGF-2 alone and the combined treated groups are significantly reduced versus the vehicle group (*P<0.05, ***P<0.001, respectively). Swimming: the combined group is significantly different from 8-OH-DPAT and FGF-2 alone groups (+++P<0.001); the groups treated with FGF-2 alone and the combined treated groups are highly significantly reduced versus the vehicle group (***P<0.001) and the FGF-2 alone group is significantly reduced versus

the 8-OH-DPAT alone group ($^{\&\&}P<0.01$). Statistical analysis was performed by one-way analysis of variance (ANOVA) followed by Tukey's Multiple Comparison post-test.

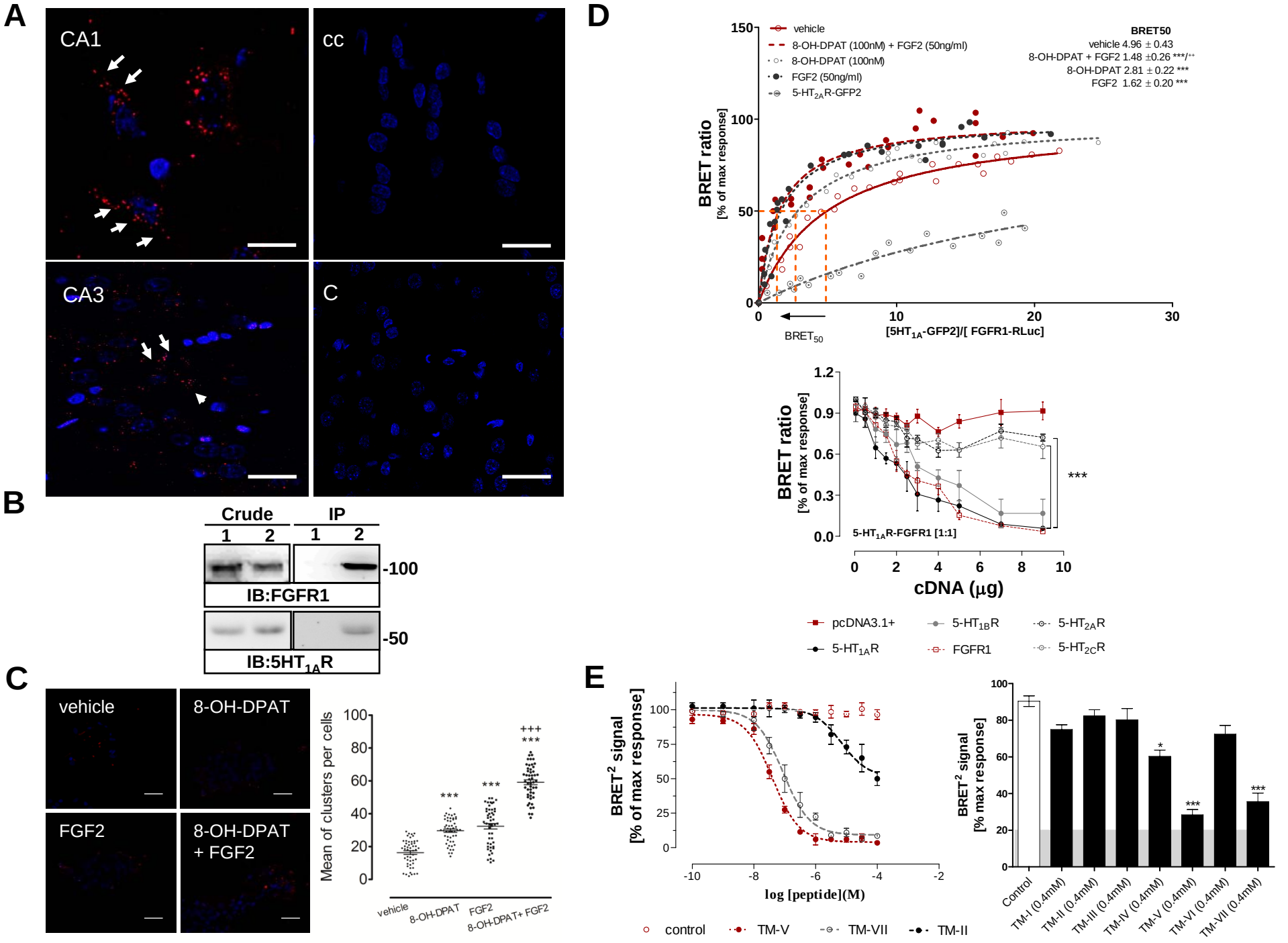
A
CA1
cc
CA3
C
B
Crude
IP
1
2
1
2
-100
IB:FGFR1
-50
IB:5HT1AR
C
vehicle
8-OH-DPAT
FGF2
8-OH-DPAT + FGF2
Mean of clusters per cells
vehicle
8-OH-DPAT
FGF2
8-OH-DPAT+ FGF2
D
vehicle
8-OH-DPAT (100nM) + FGF2 (50ng/ml)
8-OH-DPAT (100nM)
FGF2 (50ng/ml)
5-HT2AR-GFP2
BRET50
vehicle 4.96 ± 0.43
8-OH-DPAT + FGF2 1.48 ±0.26 ***/++
8-OH-DPAT 2.81 ± 0.22 ***
FGF2 1.62 ± 0.20 ***
BRET ratio
[% of max response]
BRET50
[5HT1A-GFP2]/[FGFR1-RLuc]
5-HT1AR-FGFR1 [1:1]
cDNA (µg)
pcDNA3.1+
5-HT1BR
5-HT2AR
5-HT1AR
FGFR1
5-HT2CR
E
BRET2 signal
[% of max response]
log [peptide](M)
control
TM-V
TM-VII
TM-II
Control
TM-I (0.4mM)
TM-II (0.4mM)
TM-III (0.4mM)
TM-IV (0.4mM)
TM-V (0.4mM)
TM-VI (0.4mM)
TM-VII (0.4mM)

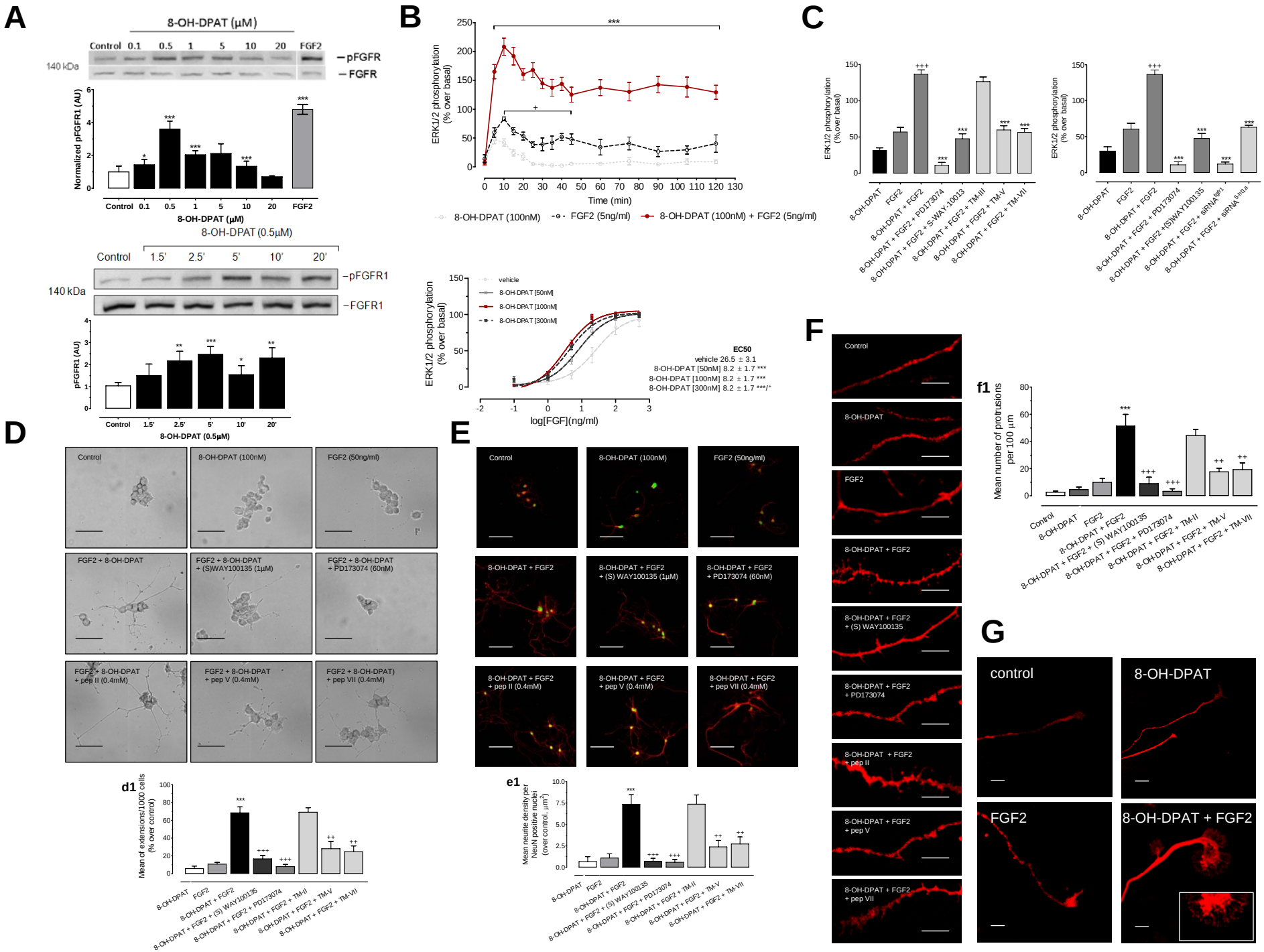
A
8-OH-DPAT (μM)
Control 0.1 0.5 1 5 10 20 FGF2
140 kDa
pFGFR
FGFR
Normalized pFGFR1 (AU)
8-OH-DPAT (μM)
8-OH-DPAT (0.5μM)
Control 1.5' 2.5' 5' 10' 20'
pFGFR1
FGFR1
pFGFR1 (AU)
8-OH-DPAT (0.5μM)
B
ERK1/2 phosphorylation (% over basal)
Time (min)
8-OH-DPAT (100nM)
FGF2 (5ng/ml)
8-OH-DPAT (100nM) + FGF2 (5ng/ml)
vehicle
8-OH-DPAT [50nM]
8-OH-DPAT [100nM]
8-OH-DPAT [300nM]
log[FGF](ng/ml)
EC50
vehicle 26.5 ± 3.1
8-OH-DPAT [50nM] 8.2 ± 1.7 ***
8-OH-DPAT [100nM] 8.2 ± 1.7 ***
8-OH-DPAT [300nM] 8.2 ± 1.7 ***/+
C
ERK1/2 phosphorylation (%over basal)
8-OH-DPAT
FGF2
8-OH-DPAT + FGF2
8-OH-DPAT + FGF2 + PD173074
8-OH-DPAT + FGF2 + S-WAY-10013
8-OH-DPAT + FGF2 + TM-III
8-OH-DPAT + FGF2 + TM-V
8-OH-DPAT + FGF2 + TM-VII
ERK1/2 phosphorylation (% over basal)
8-OH-DPAT + FGF2 + (S)WAY100135
8-OH-DPAT + FGF2 + siRNA fgfr1
8-OH-DPAT + FGF2 + siRNA 5-ht1a
D
Control
8-OH-DPAT (100nM)
FGF2 (50ng/ml)
FGF2 + 8-OH-DPAT
FGF2 + 8-OH-DPAT + (S)WAY100135 (1μM)
FGF2 + 8-OH-DPAT + PD173074 (60nM)
FGF2 + 8-OH-DPAT + pep II (0.4mM)
FGF2 + 8-OH-DPAT + pep V (0.4mM)
FGF2 + 8-OH-DPAT) + pep VII (0.4mM)
d1
Mean of extensions/1000 cells (% over control)
8-OH-DPAT
FGF2
8-OH-DPAT + FGF2
8-OH-DPAT + FGF2 + (S) WAY100135
8-OH-DPAT + FGF2 + PD173074
8-OH-DPAT + FGF2 + TM-II
8-OH-DPAT + FGF2 + TM-V
8-OH-DPAT + FGF2 + TM-VII
E
Control
8-OH-DPAT (100nM)
FGF2 (50ng/ml)
8-OH-DPAT + FGF2
8-OH-DPAT + FGF2 + (S) WAY100135 (1μM)
8-OH-DPAT + FGF2 + PD173074 (60nM)
8-OH-DPAT + FGF2 + pep II (0.4mM)
8-OH-DPAT + FGF2 + pep V (0.4mM)
8-OH-DPAT + FGF2 + pep VII (0.4mM)
e1
Mean neurite density per NeuN positive nuclei (over control, μm²)
8-OH-DPAT
FGF2
8-OH-DPAT + FGF2
8-OH-DPAT + FGF2 + (S) WAY100135
8-OH-DPAT + FGF2 + PD173074
8-OH-DPAT + FGF2 + TM-II
8-OH-DPAT + FGF2 + TM-V
8-OH-DPAT + FGF2 + TM-VII
F
Control
8-OH-DPAT
FGF2
8-OH-DPAT + FGF2
8-OH-DPAT + FGF2 + (S) WAY100135
8-OH-DPAT + FGF2 + PD173074
8-OH-DPAT + FGF2 + pep II
8-OH-DPAT + FGF2 + pep V
8-OH-DPAT + FGF2 + pep VII
f1
Mean number of protrusions per 100 μm
Control
8-OH-DPAT
FGF2
8-OH-DPAT + FGF2
8-OH-DPAT + FGF2 + (S) WAY100135
8-OH-DPAT + FGF2 + PD173074
8-OH-DPAT + FGF2 + TM-II
8-OH-DPAT + FGF2 + TM-V
8-OH-DPAT + FGF2 + TM-VII
G
control
8-OH-DPAT
FGF2
8-OH-DPAT + FGF2

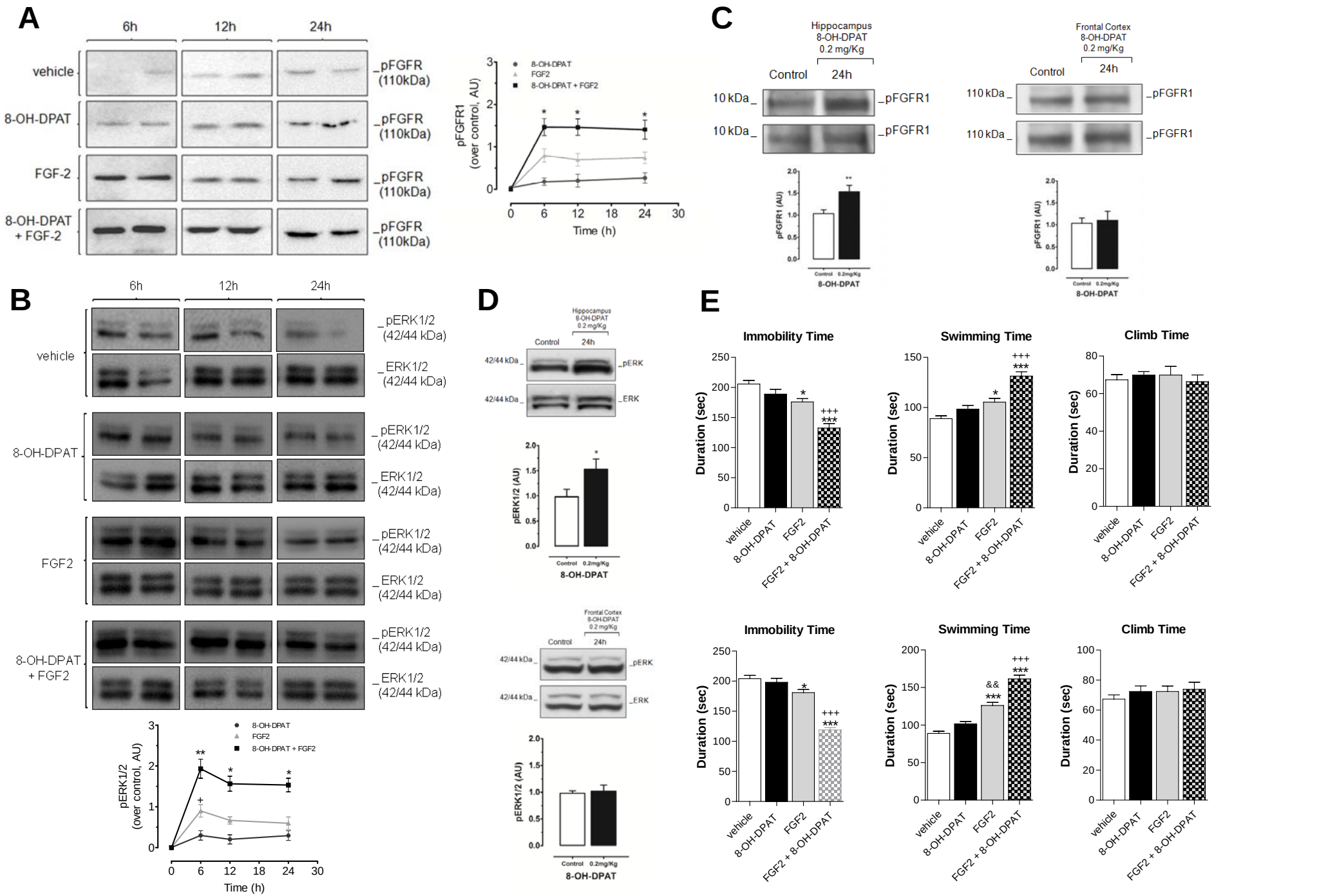
A
6h
12h
24h
vehicle
8-OH-DPAT
FGF-2
8-OH-DPAT + FGF-2
_pFGFR (110kDa)
8-OH-DPAT
FGF2
8-OH-DPAT + FGF2
pFGFR1 (over control, AU)
Time (h)
B
_pERK1/2 (42/44 kDa)
_ERK1/2 (42/44 kDa)
vehicle
8-OH-DPAT
FGF2
8-OH-DPAT + FGF2
pERK1/2 (over control, AU)
Time (h)
C
Hippocampus
8-OH-DPAT
0.2 mg/Kg
Control
24h
10 kDa
_pFGFR1
pFGFR1 (AU)
Control
0.2mg/Kg
8-OH-DPAT
Frontal Cortex
8-OH-DPAT
0.2 mg/Kg
110 kDa
D
Hippocampus
8-OH-DPAT
0.2 mg/Kg
42/44 kDa
_pERK
_ERK
pERK1/2 (AU)
8-OH-DPAT
Frontal Cortex
8-OH-DPAT
0.2 mg/Kg
E
Immobility Time
Swimming Time
Climb Time
Duration (sec)
vehicle
8-OH-DPAT
FGF2
FGF2 + 8-OH-DPAT

SUPPLEMENTARY Figure S-1

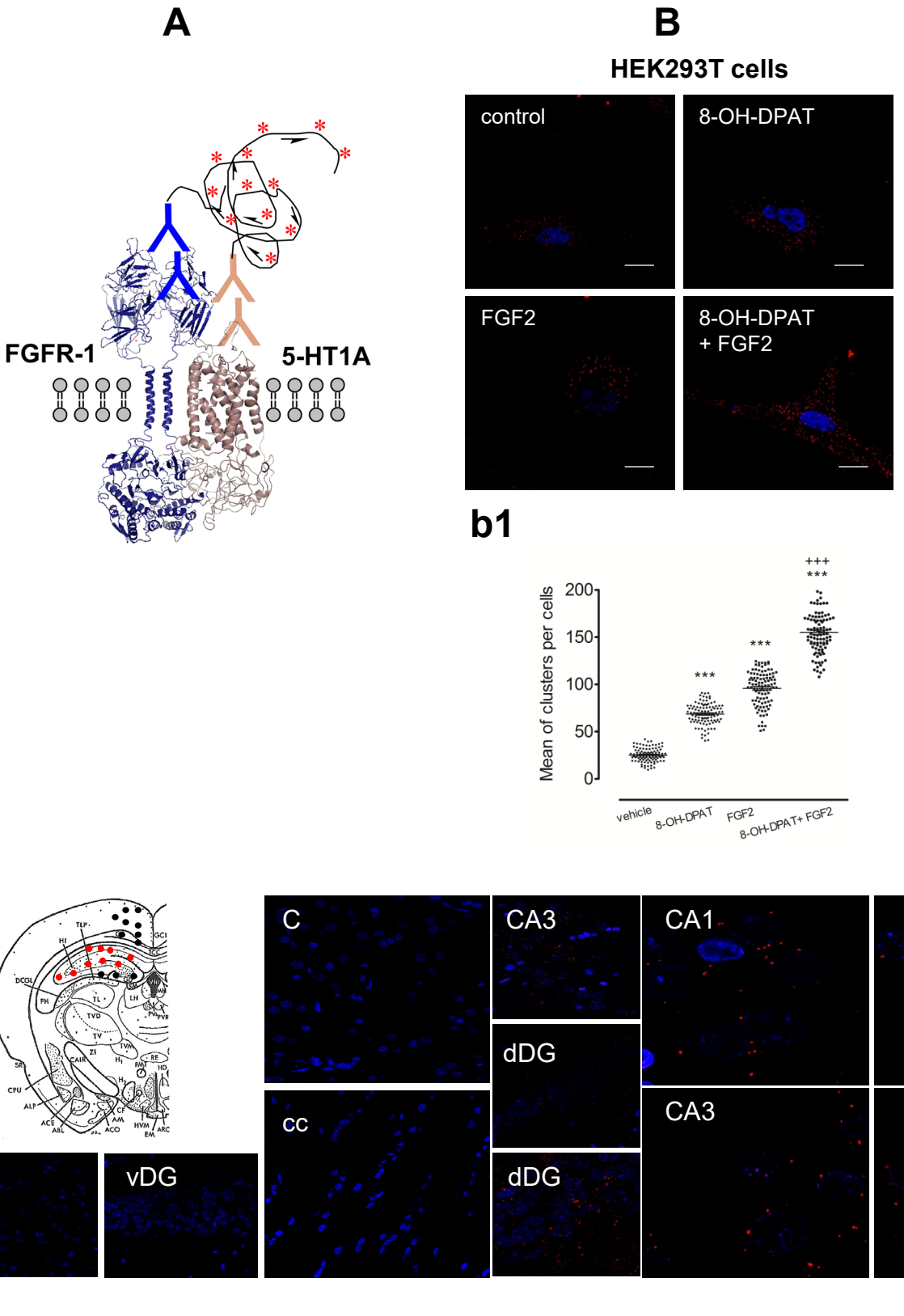

SUPPLEMENTARY Figure S-2A

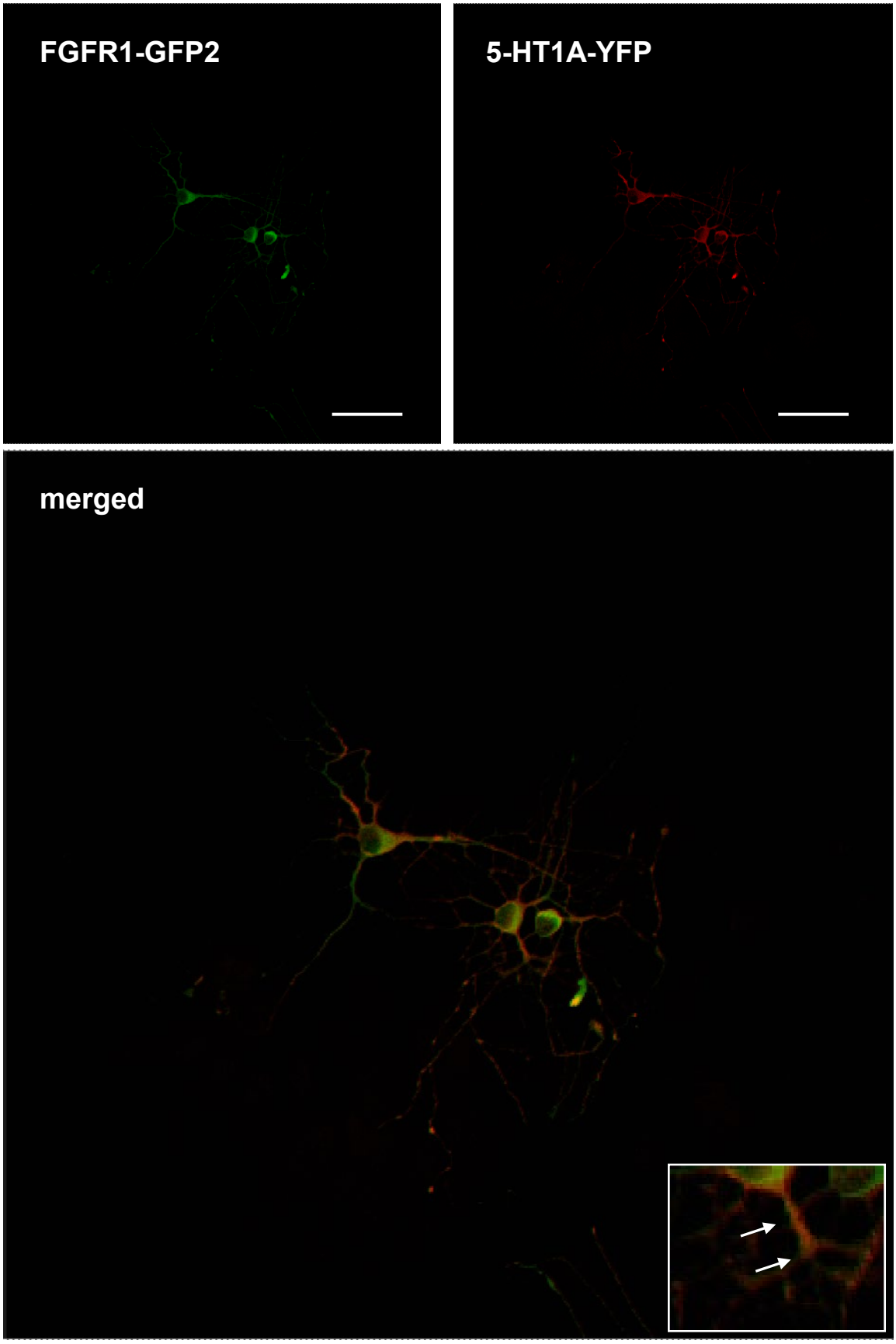

SUPPLEMENTARY Figure S-2A continuation

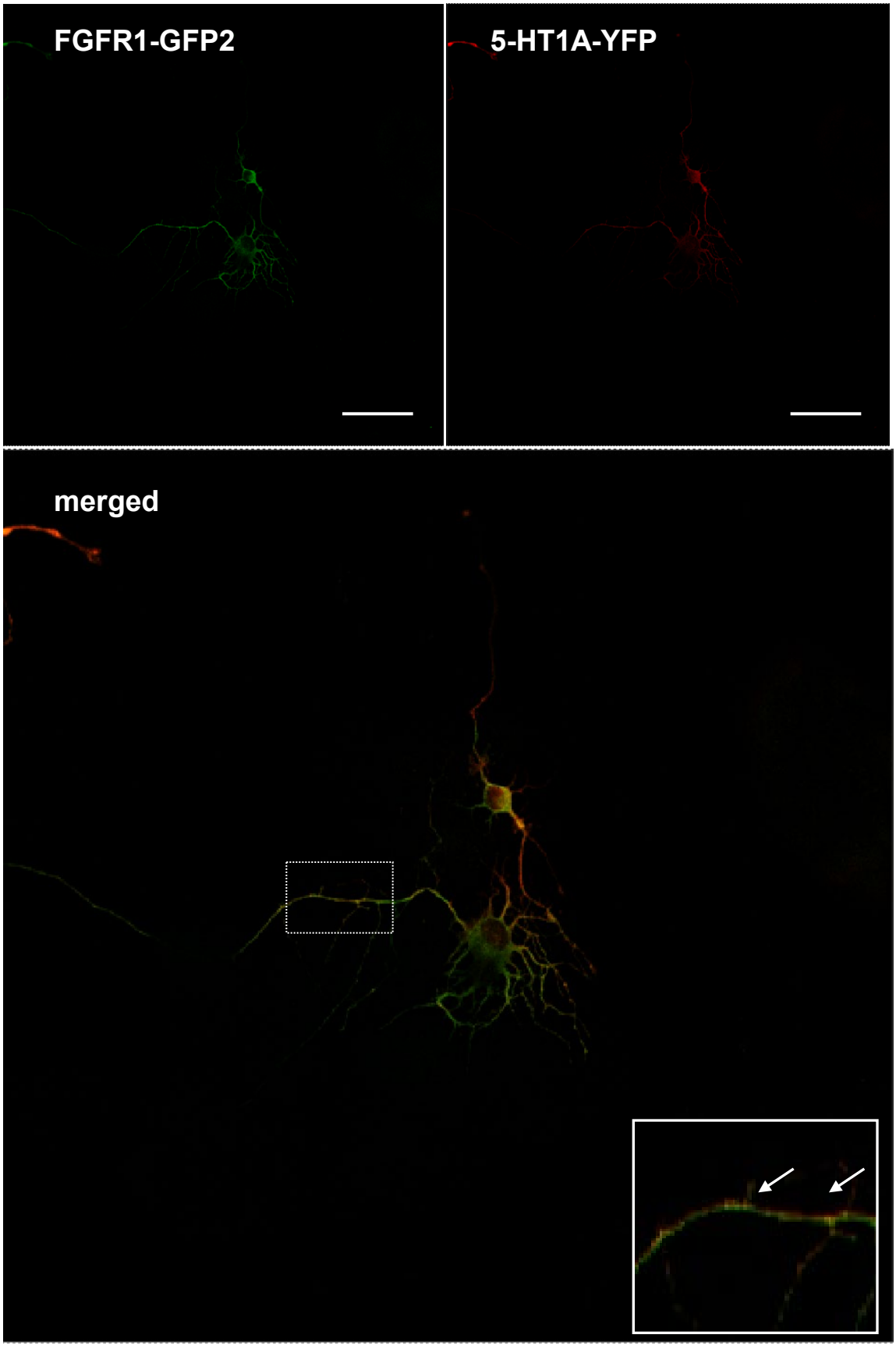

SUPPLEMENTARY Figure S-2B

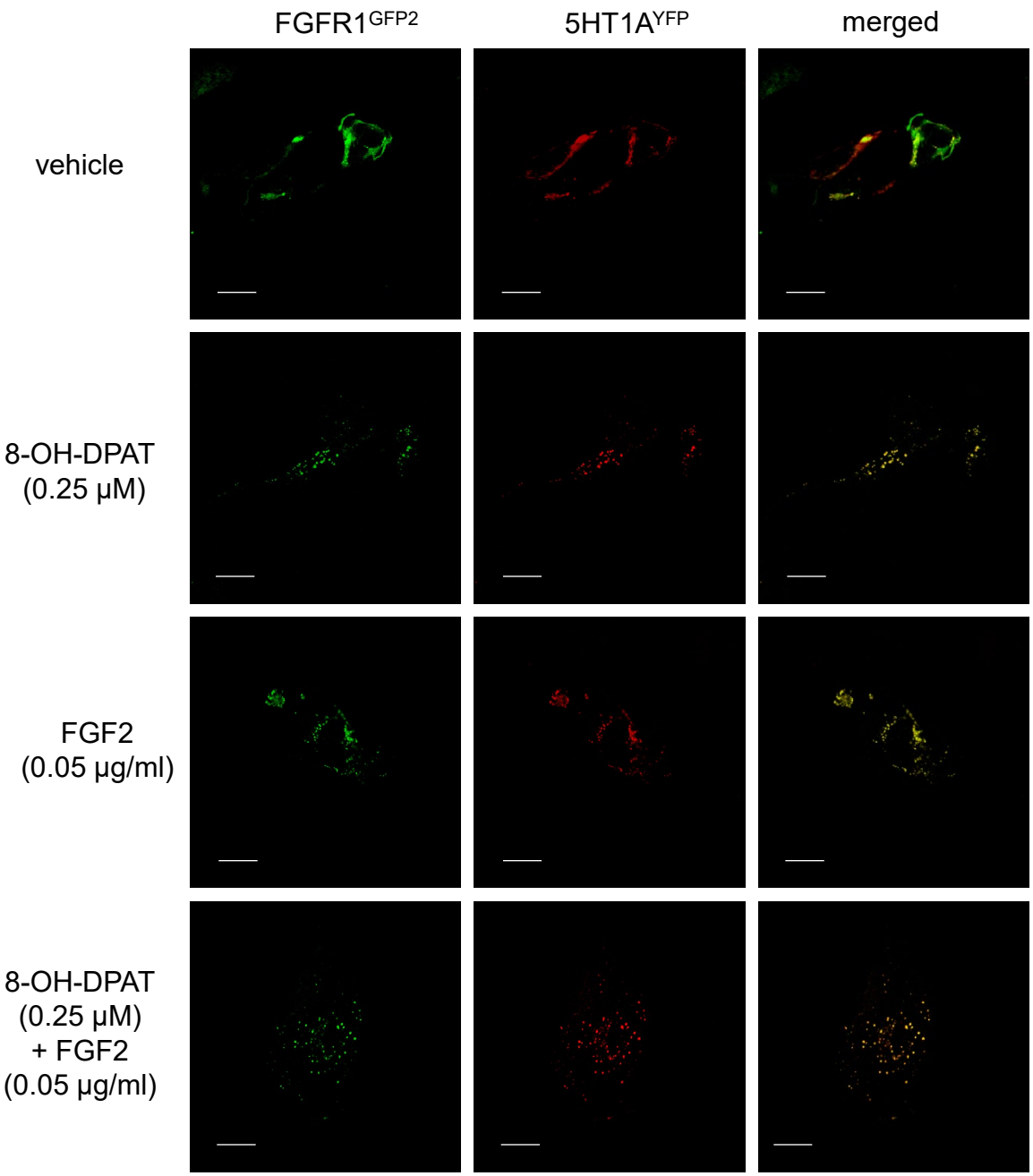

SUPPLEMENTARY Figure S-3

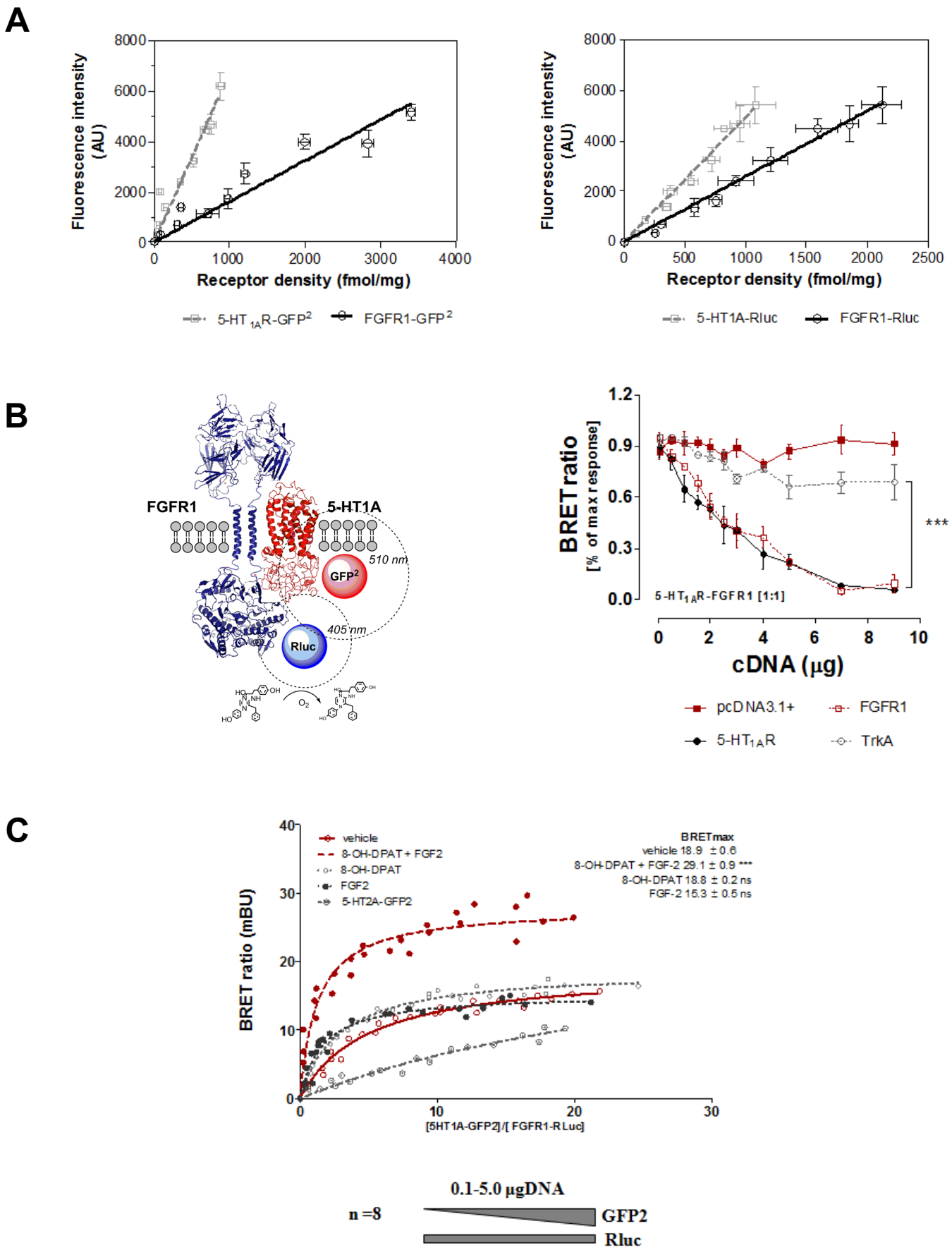

SUPPLEMENTARY Figure S-4

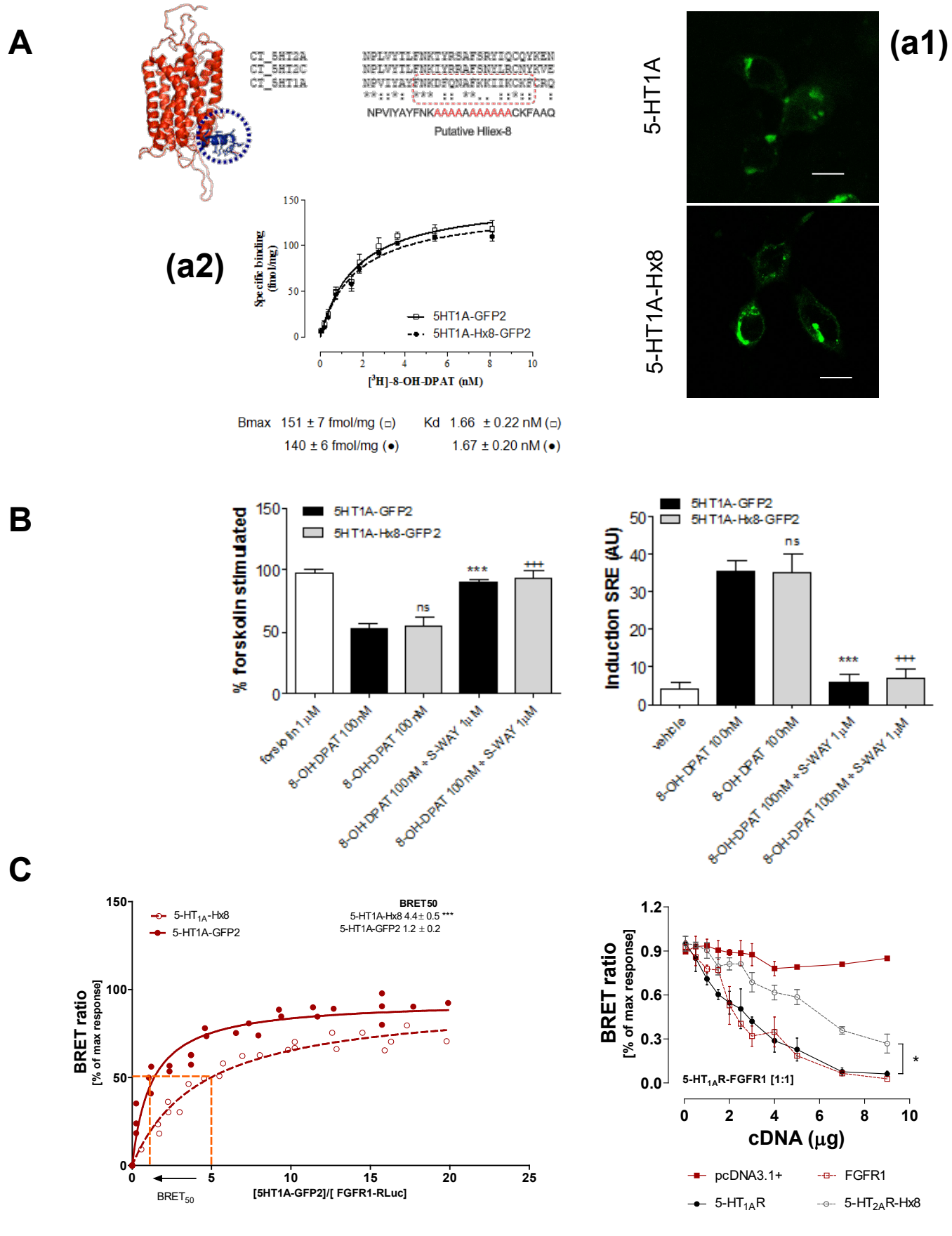

SUPPLEMENTARY Figure S-5

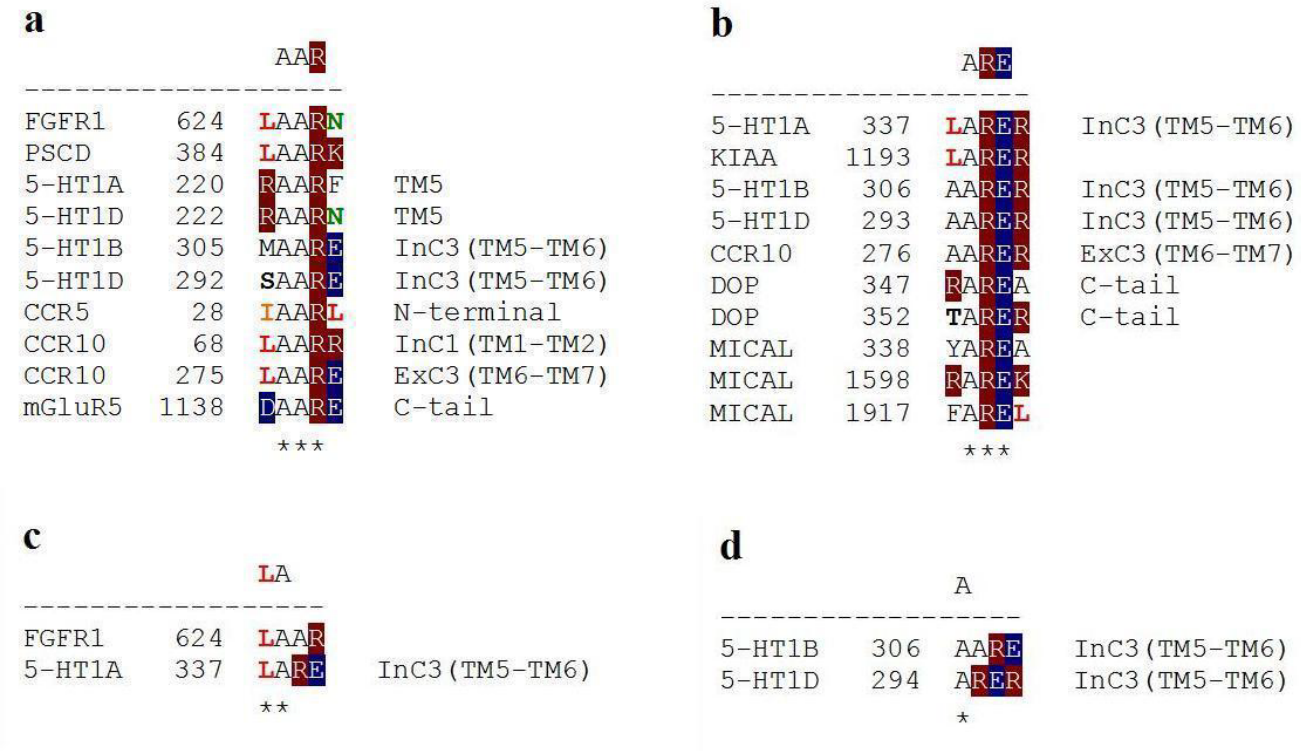

Table 1: Example of triplet homologies in receptor heteromers and HIV entry

Triplet	Rank	Receptor heteromers	HIV entry
AAR	7	A2A-D2, A2A-mGluR5, D2-mGluR5, mGluR5-GABAB1, D2-CCKBR, 5HT1B-5HT1D, MHC1-CD8	KIAA-MICAL KIAA-PSCD PSCD-MICAL
ARE	1	5HT1B-5HT1D	KIAA-MICAL

Table 2: Example of triplets (yes/no: */-) in serotonin receptors, FGFR1 and TrkB

Receptor Triplet	5HT1A	5HT1B	5HT1D	5HT2A	5HT2B	FGFR1	TrkB
AAR	*	*	*	-	-	*	-
ARE	*	*	*	-	-	-	-

SUPPLEMENTARY Figure S-6

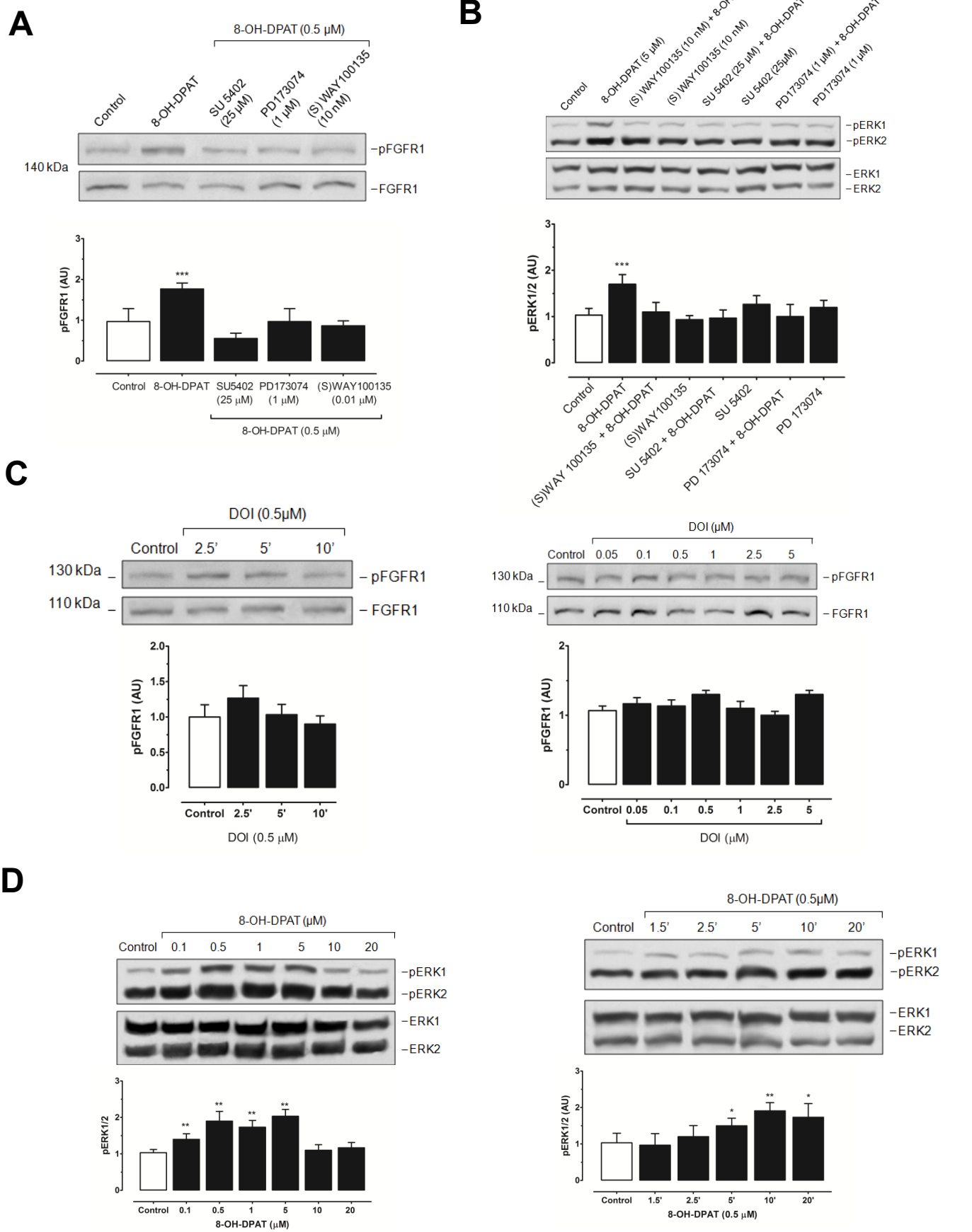

SUPPLEMENTARY Figure S-6E

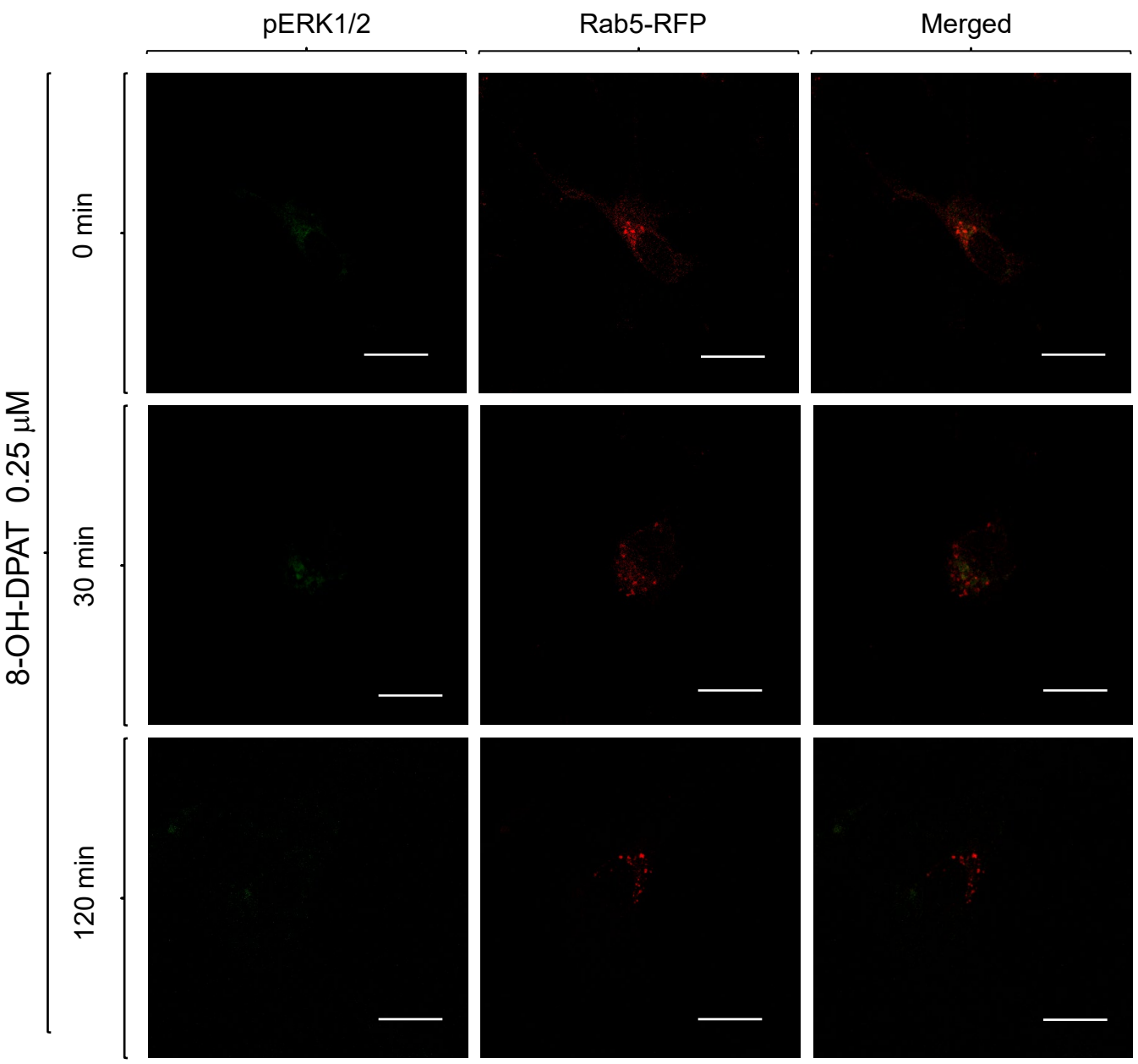

SUPPLEMENTARY Figure S-6E continuation

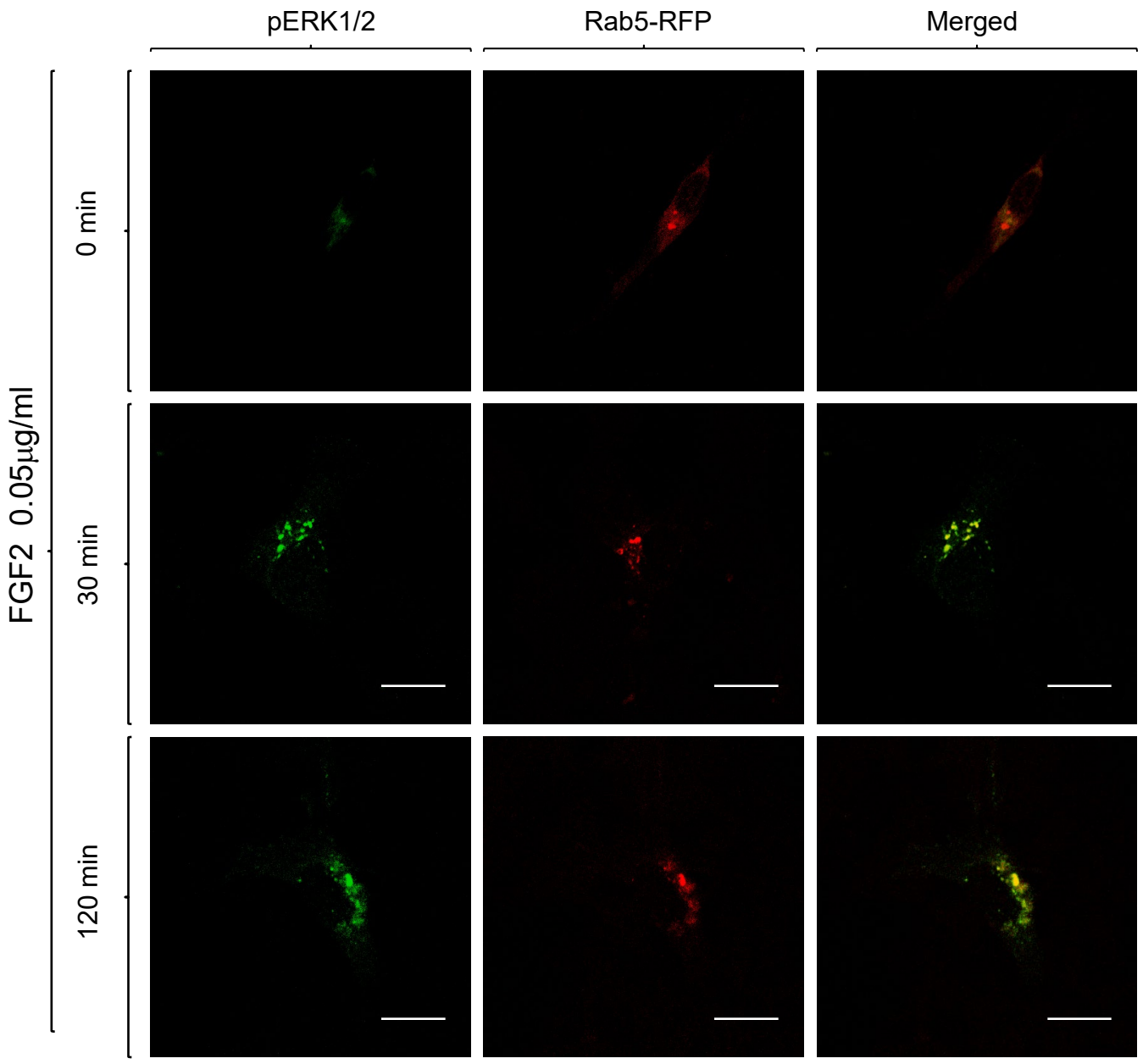

SUPPLEMENTARY Figure S-6E continuation

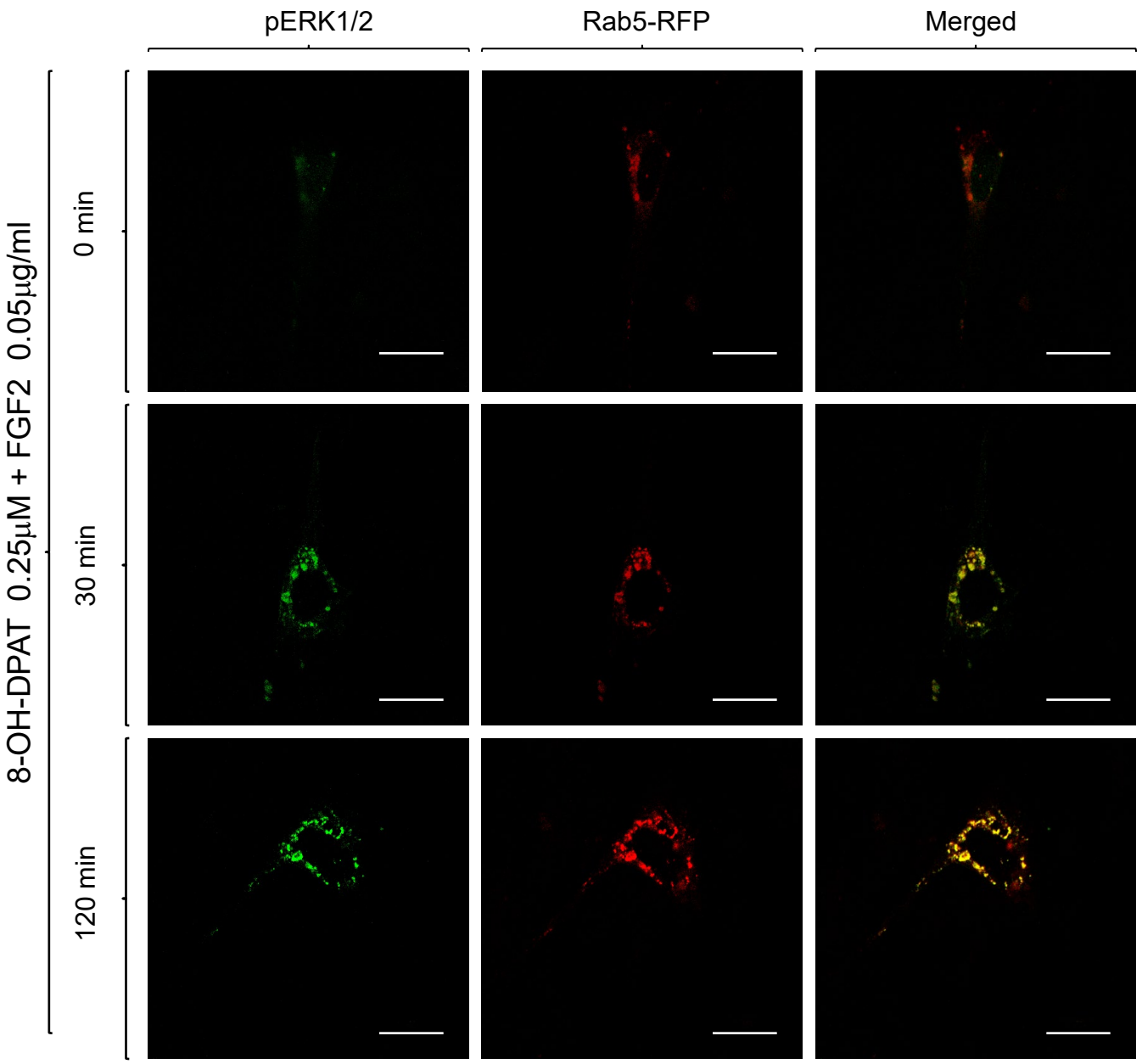

SUPPLEMENTARY Figure S-6E continuation

A

Treatment	Yellow fluorescence intensity [pERK1/2-IR(green)-Rab5-RFP]			Ratio of Yellow fluorescence intensity/ green fluorescence intensity (pERK-IR Alexa Fluor 488)		
	0 min	30 min	120 min	0 min	30 min	120 min
Vehicle	100±99	109±37	95±22	0.17±0.03	0.19±0.11	0.15±0.02
8-OH-DPAT (0.25μM)	121±18	93±52	137±41	0.19±0.04	0.15±0.03	0.19±0.03
FGF2 (0.05μg/ml)	124±40	7006±537***,&&&	6895±309***,&&&	0.12±0.07	0.37±0.08*,&	0.42±0.09*,&
8-OH-DPAT (0.25μM) + FGF2 (0.05μg/ml)	178±295	8931±656***,++	16537±322***,+++	0.11±0.02	0.51±0.07***,+	0.87±0.08***,++

B

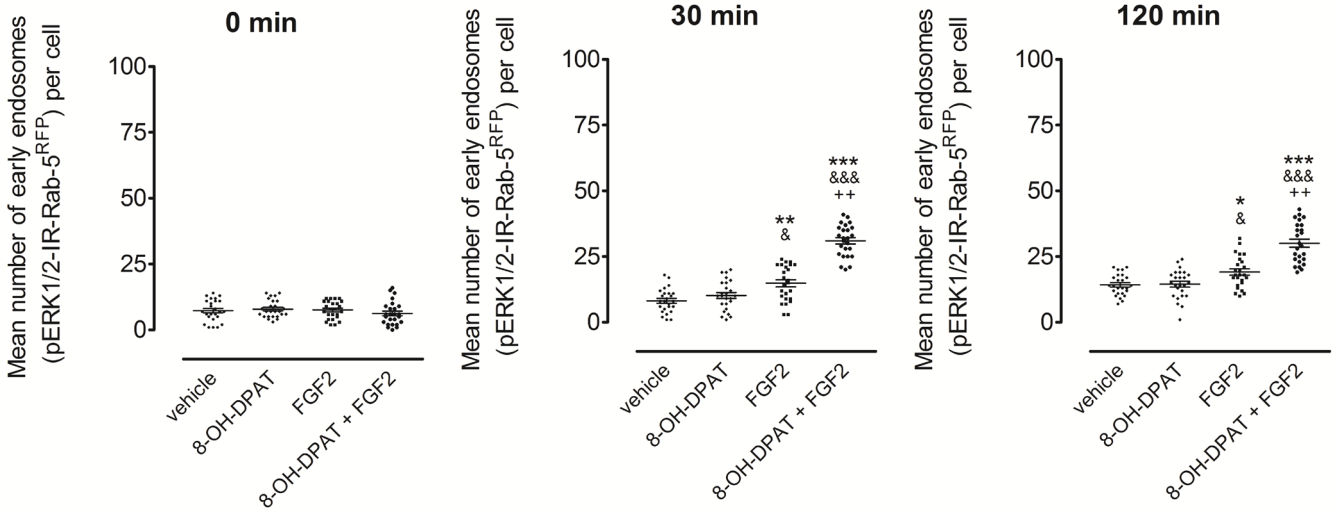

SUPPLEMENTARY Figure S-7

A

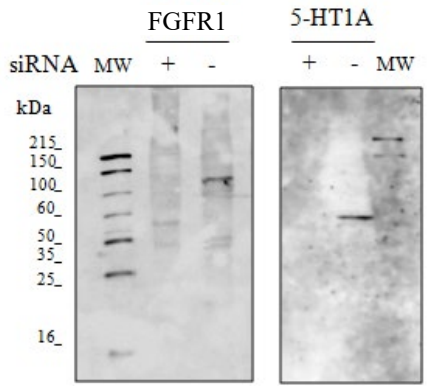

B

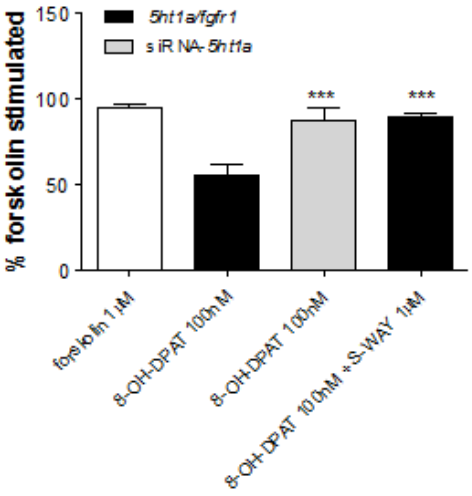

C

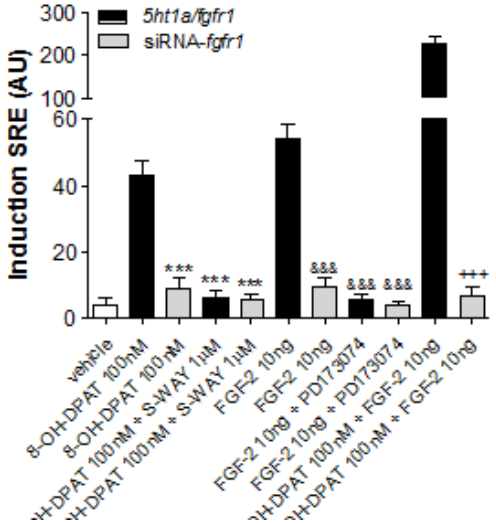

SUPPLEMENTARY Figure S-8

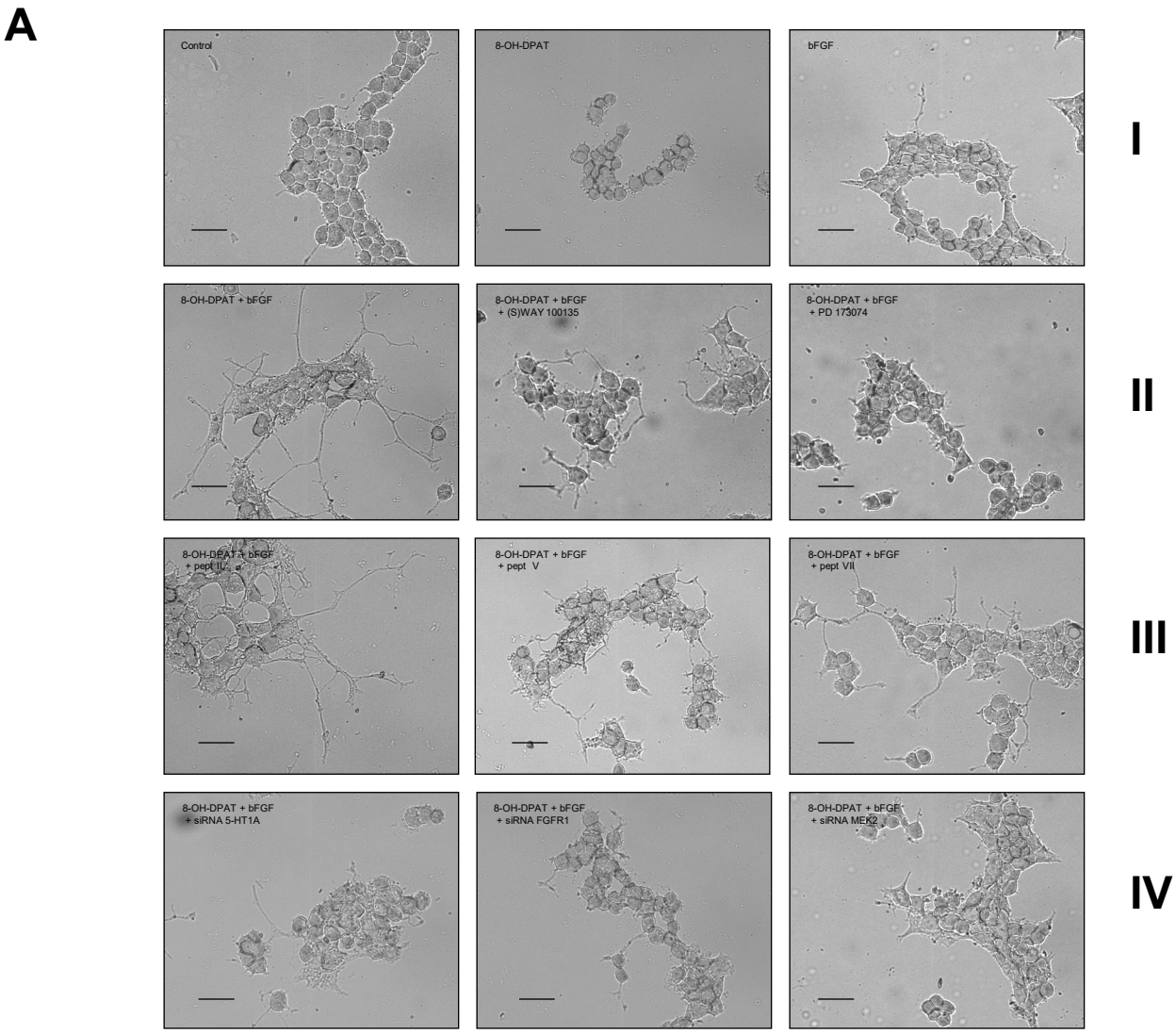

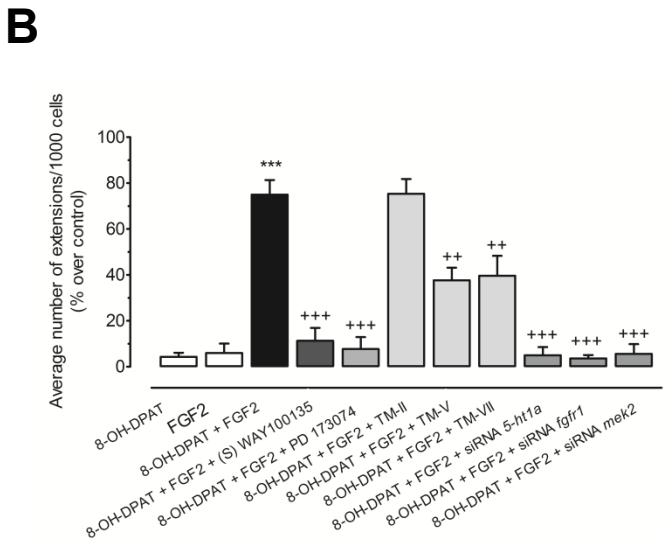

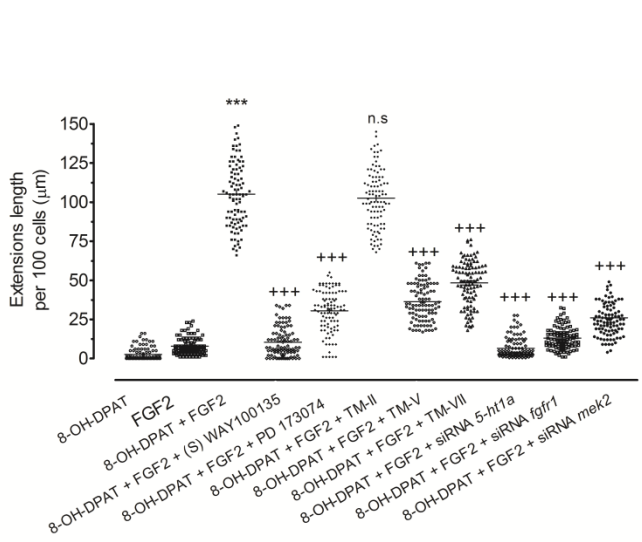

SUPPLEMENTARY Figure S-9

A

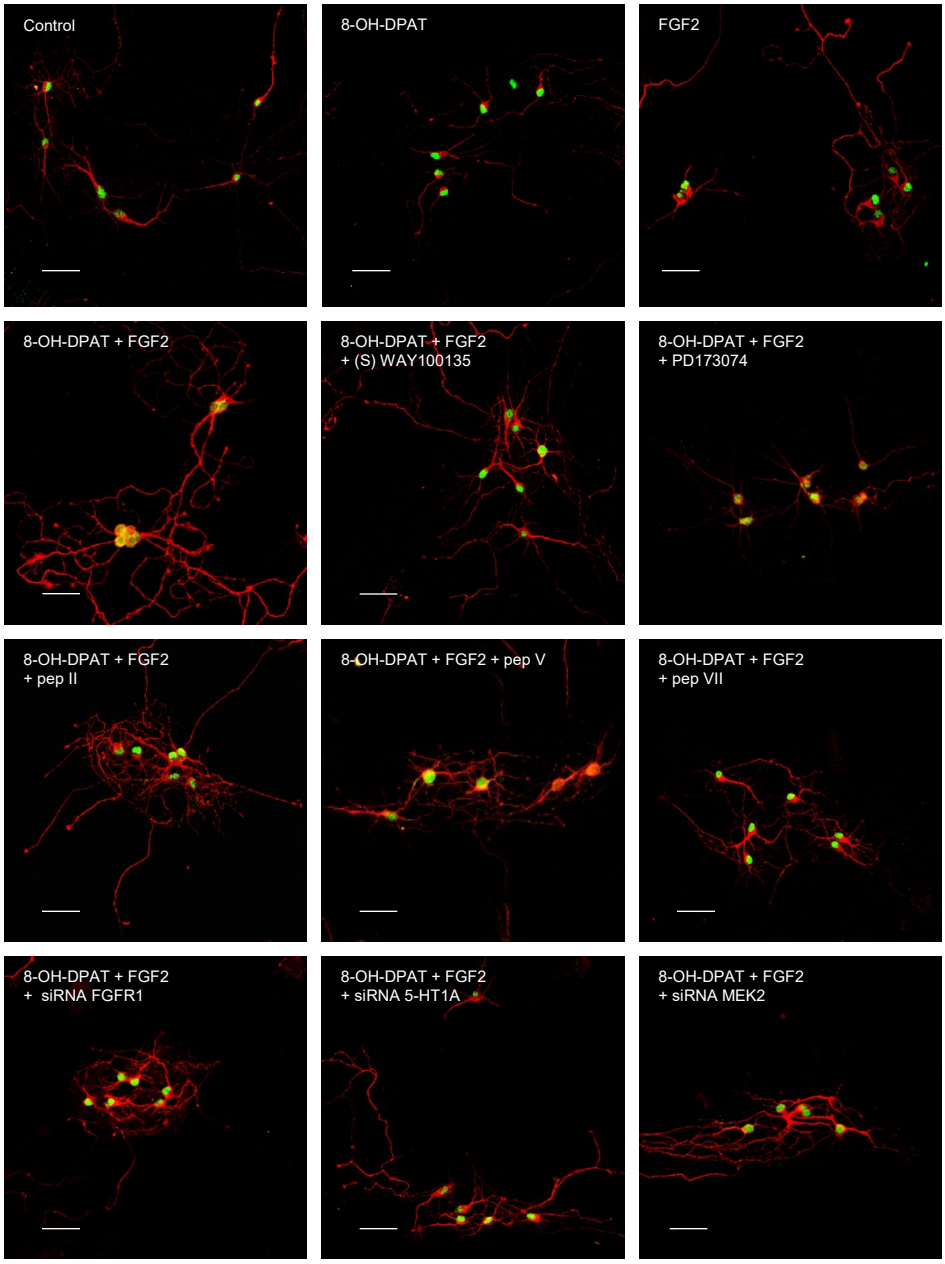

B

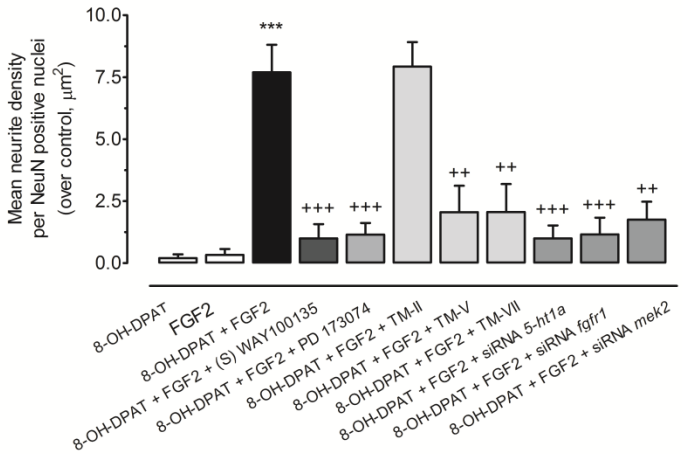

SUPPLEMENTARY Figure S-10